# BETA-HYDROXYBUTYRATE COUNTERACTS THE DELETERIOUS EFFECTS OF A SATURATED HIGH-FAT DIET ON SYNAPTIC AMPA RECEPTORS AND COGNITIVE PERFORMANCE

**Running title:** Nutrition effects on synaptic function

Rocío Rojas[1], Christian Griñán-Ferré[2,3], Aida Castellanos[4,5,6], Ernesto Griego[7], Marc Martínez[1], Juan de Dios Navarro-López[6], Lydia Jiménez-Díaz[6], José Rodríguez-Álvarez[3,8], David Soto del Cerro[4,5], Pablo E Castillo [7,9], Mercè Pallàs[2,3], Rut Fadó[1,8,10*], and Núria Casals[1,10]

[1]Basic Sciences Department, Faculty of Medicine and Health Sciences, Universitat Internacional de Catalunya, E-08195 Sant Cugat del Vallès, Spain.

[2]Department of Pharmacology, Toxicology and Therapeutic Chemistry, School of Pharmacy and Food Sciences, University of Barcelona, Joan XXIII 27-31, 08028, Barcelona, Spain.

[3]CIBER Enfermedades Neurodegenerativas (CIBERNED), Instituto de Salud Carlos III (ISCIII), Madrid, Spain.

[4]Laboratory of Neurophysiology, Department of Biomedicine, Faculty of Medicine and Health Sciences, Institute of Neurosciences, University of Barcelona, Barcelona, Spain

[5]August Pi i Sunyer Biomedical Research Institute (IDIBAPS), Barcelona, Spain

[6]Neurophysiology & Behaviour Laboratory, Regional Centre for Biomedical Research (CRIB), Faculty of Medicine of Ciudad Real, University of Castilla-La Mancha, Ciudad Real, Spain

[7]Dominick P. Purpura Department of Neuroscience, Albert Einstein College of Medicine, New York, New York 10461.

[8]Institut de Neurociències, Universitat Autònoma de Barcelona, 08193 Bellaterra, Cerdanyola del Vallès, Spain.

[9]Department of Psychiatry & Behavioral Sciences, Albert Einstein College of Medicine, New York, New York 10461.

[10]Centro de Investigación Biomédica en Red de Fisiopatología de la Obesidad y la Nutrición (CIBEROBN), Instituto de Salud Carlos III, E-28029 Madrid, Spain.

*Corresponding author at Universitat Internacional de Catalunya, E-08195 Sant Cugat del Valles, Spain. E-mail address: ncasals@uic.es (N.C.) and rfado@uic.es (R.F.)

***Abstract***

The ketogenic diet, high-fat and low-carbohydrates, has witnessed a significant rise in popularity, not merely as a bodyweight management strategy but also as a regimen that demonstrated efficacy in delaying cognitive decline associated with neurodegenerative diseases and the aging process. This dietary approach triggers the liver's production of ketone bodies, mainly β-hydroxybutyrate, used as an alternative energy source for neurons, crucial for maintaining glutamatergic synapses. However, it remains to be established whether β-hydroxybutyrate can counteract impaired AMPA receptor trafficking, synaptic dysfunction, and cognitive decline induced by metabolic challenges like saturated fatty acids. Here, we report that palmitic acid, a saturated fatty acid, decreased surface glutamate GluA1-type AMPA receptor levels in cultured cortical neurons, while the unsaturated fatty acids (oleic acid and ω-3 docosahexaenoic acid) and β-hydroxybutyrate increased them. Furthermore, this ketone body counteracted the adverse effects of palmitic acid on synaptic GluA1 levels and synaptic transmission, excitability, and plasticity. Again, daily intragastrical administration of β-hydroxybutyrate for two months was able to reverse the cognitive impairment mediated by a saturated high-fat diet in a mouse experimental model. Overall, our findings not only support the pivotal role of nutrients on synaptic function and neuroplasticity but provide novel insights into the potential of β-hydroxybutyrate to delay cognitive impairments linked to metabolic diseases.

**Keywords:** beta-hydroxybutyrate, palmitic acid, oleic acid, docosahexaenoic acid, AMPA receptor, GluA1, saturated high-fat diet, memory.

## Introduction

The escalating prevalence of cognitive impairment and dementia, projected to reach 150 million cases by 2050, represents a severe global public health concern [1]. While increased life expectancy contributes to this outcome, attention has shifted to the impact of nutrition on brain health [2]. The consumption frequency of specific dietary components, such as fatty acids, influences cognition, correlating with better or worse performance in older adults [3]. The surge in obesity cases, reaching 650 million globally in 2016 [4], influenced by the consumption of high-fat/high-sugar diets, overeating behaviors, and sedentary lifestyles, heightens the risk of dementia in later life [5]. Moreover, obesity has been associated with altered cognitive performance [6], although the precise physiopathological mechanisms are not yet fully understood.

Cognitive performance is variably affected by different fat types [7]. Regular consumption of unhealthy saturated fats (SFA), solids fats primarily derived from animals, such as meat and dairy, and trans fats, liquid oils solidifying after food processing, has been associated with impaired memory performance, particularly in both young and old populations [8–10]. By contrast, dietary supplementation with polyunsaturated fatty acids (PUFAs) has shown the potential to decelerate cognitive decline in Alzheimer's disease (AD) patients [11]. Interestingly, adherence to the Mediterranean diet, known for its richness in omega-3 (ω-3) PUFAs and oleic acid (OA), has been associated with a reduced risk of cognitive impairment and dementia in patients with AD or even with established Metabolic Syndrome [12,13].

Neuroplasticity drives the formation and adjustment of synaptic connections during learning and memory tasks, particularly within hippocampal glutamatergic circuits [14]. This fact involves precise control over the α-amino-3-hydroxy-5-methyl-4-isoxazolepropionic acid (AMPA)-type glutamate receptors (AMPARs) in the post-synaptic zone (PSZ). AMPARs are tetrameric assemblies of GluA1-4 subunits, consisting of two GluA1/GluA2 dimers that are $Ca^{2+}$-impermeable in mature neurons under resting conditions. GluA1-GluA1 homomers are incorporated at the plasma membrane (PM), forming Ca2+-permeable receptors (CP-AMPARs) upon glutamate stimulation. This controlled CP-AMPAR inclusion supports synaptic potentiation during neuroplasticity. Dysregulation of AMPAR subunit expression or trafficking imbalance toward the surface can impact synaptic function, influencing cognitive processes [15].

Indeed, the impact of various fats on cognitive function is closely associated with alterations in synaptic function, plasticity, and modifications in synaptic AMPARs [7], as evidenced *in vivo* using animal models and *in vitro* with slices and cultured neurons. Diets rich in saturated fatty acids (SFAD) resulted in diminished spine density and narrowed PSD in the hippocampus (HPC) [16]. Treatment with saturated palmitic fatty acid (PA) reduced dendritic arborization and induced synaptic loss in HPC neurons, and both effects were successfully counteracted when co-treated with the primary ω-3 docosahexaenoic acid (DHA) [17][18]. Exposure to SFAD increased PA deposition, leading to hyper-palmitoylation and hypo-phosphorylation of GluA1 [19]. Furthermore, co-treatment with PA and insulin diminished the recruitment of GluA1 at the PM and inhibited AMPAR-mediated currents *in vitro*. By contrast, ω-3 PUFAs positively regulate synaptic function and GluA1 levels within HPC synaptosomes, while ω-6 PUFAs exhibit either no effect or negative impact; studies on OA alone lack sufficient data for conclusions [7].

Recent work indicates that ketogenic diets (KD), high in fats and low in carbohydrates, and ketone bodies (KBS) produced during KD or fasting by the liver, mitigate cognitive decline associated with aging and neurodegeneration [12]. Additionally, ketogenic formulas prevent memory deficits induced by hypoglycemia in type 1 diabetic patients [20], while the administration of β-hydroxybutyrate (BHB), the primary KB, improves working memory in type 2 patients [21]. However, their impact on synaptic function, neuroplasticity, and AMPARs regulation remains incomplete. Here, we explored whether BHB can mitigate the adverse effects of saturated fatty acids on AMPAR trafficking, synaptic plasticity, and cognition. Our results indicate that BHB prevented the surface withdrawal of GluA1 induced by PA in hippocampal neurons *in vitro*. In HPC slices, BHB co-treatment counteracted the PA-mediated decrease in excitability and plasticity. In SFAD-fed mice, daily intragastrical administration of BHB prevented diet-induced cognitive impairment, highlighting the potential of this ketone body in mitigating the detrimental effects of unhealthy nutrition on brain function.

## Results

### *Nutrients' impact on surface levels of GluA1 in cortical neurons*

Given the pivotal role of GluA1 abundance on the neuronal surface in shaping synaptic plasticity, we explored the influence of saturated (PA) and unsaturated (OA and DHA) on the levels of GluA1 at the PM. Furthermore, the effects of the major ketone body, BHB, which is synthesized by the liver in fasting situations or under high-fat, low-carbohydrates diets, were also analyzed.

For this purpose, mouse primary cortical neurons cultured along 13-14 DIV were treated with either PA (200µM), OA (200µM), DHA (200µM), BHB (5mM) or vehicle (0.6% BSA) in two distinct regimens: a brief exposure lasting 2 hours and a prolonged exposure spanning 24 hours. Then, we analyzed GluA1 levels on the PM by immunocytochemistry in nonpermeabilized cells using an antibody against its N-terminal extracellular domain.

The results showed that the exposure of cortical cultures to the saturated fatty acid palmitate triggered the removal of GluA1 from the PM (Fig. 1A-B), even for a short-term treatment. In contrast, the treatment with the monounsaturated fatty acid oleate or with the polyunsaturated fatty acid DHA, the most prevalent ω-3 fatty acid in the brain, increased the surface levels of GluA1 in cortical neurons (Fig. 1C-F), with significantly more pronounced effects with longer exposures. Likewise, the administration of the

ketone body BHB produced the same effect (Fig. 1G-H). However, in this case, a mere 2-hour treatment was enough to enhance the surface levels of GluA1 markedly.

Additionally, the effects of these nutrients were examined using an alternative experimental model: the human-derived SH-SY5Y neuroblastoma cells. This cell line can be differentiated into a neuron-like phenotype by the exposition of retinoic acid, which promotes the growth of neurites. In this context, the treatment of differentiated SH-SY5Y with PA, OA, DHA, or BHB for 24 hours was able to recapitulate the same effects observed in cultured cortical neurons (Suppl. Fig. 1.). Therefore, these neuron-like cells could be a suitable alternative model for studying the impact of these nutrients, avoiding the use of animals.

These results confirm a distinct impact of PA, OA, DHA, and BHB on GluA1 surface levels. In addition, each nutrient showed a more substantial effect with the long-term treatment than the shorter one.

***Synaptic transmission is reduced in palmitate-treated cortical neurons.***

To explore the potential impact of nutrient-mediated regulation of surface GluA1 on synaptic transmission, AMPAR-mediated miniature excitatory postsynaptic currents (mEPSCs) were measured in primary cortical neurons following the exposure to nutrients. Henceforth, the following experiments were conducted with PA and BHB, as these two nutrients exhibited the most significant influence regulating surface GluA1. During the recordings, the addition of D-AP5 and picrotoxin (PTX) to block N-methyl-D-aspartate (NMDA) and gamma-aminobutyric acid ($GABA_A$) receptors enabled the analysis of the currents exclusively induced by AMPAR.

AMPAR-mediated mEPSCs amplitudes were reduced in cortical neurons treated with palmitate for 24 hours, with no observable changes in the case of BHB (Fig. 2A-C). Cumulative amplitude histograms revealed a noteworthy shift in the amplitude distribution towards smaller values under PA treatment (Fig. 2D), indicating a decrease in the number of postsynaptic AMPARs. However, no significant differences were detected in the frequency of mEPSCs (Fig. 2E). This observation suggests the absence of presynaptic alterations in neurons treated with either palmitate or BHB. Similarly, the kinetic parameters, including rise time and τ-weighted, were unaffected by these treatments (Fig. 2F.G), proving that AMPAR subtype composition remained unchanged. Therefore, PA targets postsynaptic AMPARs, decreasing their abundance but not affecting their subunit composition, consequently impacting AMPAR-mediated currents. Concerning BHB, the absence of changes in mEPSCs recordings suggests

that its increase in surface GluA1 might be restricted to the perisynaptic region, a population of CP-AMPARs that might be rapidly and transiently recruited to synapses under certain conditions [22].

***BHB mitigates palmitate-mediated decrease in synaptic GluA1 levels in hippocampal neurons.***

Given the increase of surface GluA1 levels under BHB treatment, we aimed to explore whether BHB could prevent PA-induced synaptic changes; we examined the effects of their co-treatment on GluA1 synaptic abundance by colocalizing this receptor with PSD95, used as a postsynaptic density marker. Furthermore, we tested various concentrations of BHB (1 mM, 2 mM, and 5 mM), all falling within the physiological range observed in mice [23]. Here, mouse primary hippocampal cultures were employed to assess whether this neuronal type replicated the outcomes observed in cortical ones.

As expected, short-term exposition to palmitate reduced GluA1 surface levels in hippocampal neurons (Suppl. Fig. 3A), as well as the amount of synaptic GluA1 (Fig. 3; red bar). In contrast, BHB did not affect synaptic GluA1 abundance at any of the assessed concentrations (Fig 3.; green bars), although surface GluA1 increased with 5 mM of BHB (Suppl. Fig 3B), as observed previously in cortical neurons. These data align with the results of the mEPSC, where palmitate, but not BHB, induces alterations in AMPA currents. Then, hippocampal neurons were co-treated with both nutrients to analyze whether BHB could counteract the detrimental impact of PA on synaptic GluA1. Fig. 3 (blue bars) shows that,1 mM and 2 mM of BHB effectively mitigated the adverse effects of PA on synaptic GluA1, whereas 5 mM of BHB did not exhibit a significant beneficial impact. These findings suggest that the harmful effects of saturated fatty acids on GluA1 synaptic abundance could be prevented through the co-administration of ketone bodies.

***BHB restores the synaptic plasticity damage induced by palmitate in hippocampal slices.***

To explore whether the beneficial effects of BHB following PA treatment extend to the preservation of synaptic plasticity, field-EPSPs recordings were conducted in hippocampal slices. Schaffer collaterals were stimulated for these electrophysiological studies, and CA1 pyramidal neurons were recorded in the presence of PTX to block $GABA_A$ receptors.

First, to test the effect of PA and BHB on basal synaptic transmission, input/output curves were conducted by increasing stimulation intensity (from 10 to 90 V) in hippocampal slices following short-term exposition to PA, BHB or a combination of both. Our results revealed a significant reduction in the slope of input/output curves under PA treatment compared with control slices (Fig. 4A-B). In contrast, BHB administration increased this parameter. Remarkably, PA and BHB co-administration demonstrated the BHB's ability to counteract the detrimental effects induced by PA, a phenomenon observable in the superimposed field-EPSP traces.

To analyze synaptic plasticity, a stable 15-minute baseline of was established, followed by the induction of a long-term potentiation (LTP) protocol using two trains of bursts (100 pulses at 100 Hz with a 10-second interval). BHB had no significant effect on the LTP magnitude (Fig. 4C). In contrast, PA reduced the LTP magnitude, an effect successfully mitigated by the simultaneous administration of BHB. This outcome was further reflected in the representative traces (Fig. 4D), which depict the baseline before LTP (thin line) and the final 5 minutes of the time course of LTP induction (thick lines).

To test whether nutrient-mediated modulation of synaptic plasticity had a presynaptic origin, we measured the paired-pulse ratio (PPR), a metric linked to the probability of vesicular release at the synapse. PPR was unaffected across all analyzed conditions (Suppl. Fig. 4A-C), strongly suggesting that the effects of PA and BHB were exclusively postsynaptic.

Finally, to confirm that nutrient-induced effects on synaptic plasticity are attributable to AMPARs, we calculated the AMPA/NMDA ratio by comparing the amplitudes of EPSCs mediated by AMPA and NMDA receptors, respectively. PA significantly reduced the AMPA/NMDA ratio, whereas BHB induced a modest upward trend (Fig 4E-G). These results suggest that the PA-mediated effect in synaptic transmission is likely due to a reduction in AMPARs but not NMDARs.

In summary, saturated fatty acids and ketone bodies affect postsynaptic functions rather than presynaptic mechanisms. Particularly, BHB exhibited the ability to counteract the impartment caused by palmitate, restoring neuronal excitability and synaptic plasticity. Moreover, our findings point out that PA effects are mediated through AMPARs.

***BHB counteracts the cognitive impairment mediated by a saturated high-fat diet in mice.***

To assess whether the beneficial effects of BHB extend to mitigating palmitate-induced cognitive impairment, we conducted *in vivo* experiments in mice. Specifically, we explored whether daily administration of BHB could counteract the adverse effects of a saturated high-fat diet on memory task performance. To achieve this, 5 weeks-old mice were fed either a SFAD (constituting 49% of calories from saturated fat) or a standard diet (SD; 10% of calories from fat) for 7 weeks. Throughout this period, BHB (100 mg/kg/day) or an equal volume of vehicle (water) was intragastrically administrated. This dosage improved BHB levels within the HPC, reaching a maximum within 4 hours post-administration (Suppl. Fig. 5A). Body weight and food intake were monitored weekly. Finally, behavior tests were performed, and the animals were euthanized to obtain brain tissues, as illustrated in the experimental setup (Fig. 5A).

To confirm that oral gavage administrated BHB reached the brain, BHB levels were measured in the cortical region. As depicted in Figure 5B, the cortex exhibited elevated BHB levels in animals administered with BHB compared to those receiving the vehicle. These differences are significant in the high-fat diet-fed animals.

Throughout the experiment, the analysis of body weight evolution revealed a tendency for males, not females, to exhibit higher weight when subjected to a SFAD. However, this difference only reached statistical significance from weeks 5 to 7 (Fig. 5C-D). Notably, mice fed with SFAD and supplemented with BHB did not display this observed trend. The cumulative food intake increased uniformly in all the evaluated conditions (Suppl. Fig. 5B), indicating that neither the administration of BHB nor the potentially heightened palatability of the SFAD had any notable impact on overall food consumption. Nevertheless, while both groups fed with SFAD exhibited higher calorie ingestion (4.9kcal/g versus 3.8kcal/g in SD; Suppl. Fig. 5C), the administration of BHB did not correlate with a subsequent increase in body weight in male mice, supporting its protective effects at the metabolic level.

Next, as an approximation to measure GluA1 surface levels, the amount of phosphorylated GluA1 at S845 was evaluated by Western blot in dissected hippocampi. It has been demonstrated that phosphorylation at this residue, which only accounts for 0,1% of total GluA1 [24], leads is associated with the translocation of GluA1 to the PM [20] and that SFAD-feeding induces a reduction in p(S845)-GluA1 levels [17]. Additionally, total GluA1, the GluA2 subunit of AMPAR, and the GluN2A subunit of NMDAR were also analyzed. In our mice, the overall levels of the analyzed proteins remained constant across all experimental conditions (Suppl. Fig. 6A-E), even

though a marginal reduction was observed in p(S845)-GluA1 in mice treated with SFAD.

Finally, to examine the effect of SFAD and BHB administration on cognitive performance, two behavior tests were conducted at the end of the experiment: NORT and OLT. In NORT, short-term memory (2 hours post-habituation) and long-term memory (24 hours later) were assessed using the discrimination index (DI), a metric reflecting the animal's ability to recognize and remember a previously encountered object. While no significant differences were observed among SD-fed groups, mice exposed to SFAD exhibited substantial cognitive impairments completely reversed by concurrent BHB administration (Fig. 6A-B). In the assessment of spatial learning evaluated through OLT, a high difference was found between SD and SFAD (Fig. 6C), corroborating the detrimental effects of saturated fats on brain functions. Once more, the co-administration of BHB demonstrated its efficacy in counteracting the harmful impact of SFAD. In the context of this test, the examination of locomotor activity revealed that, when administered with SFAD, BHB increased the distance traveled by mice compared to the other experimental groups (Fig. 6D), suggesting heightened locomotor activity or exploration behavior. By contrast, there were no differences in the number of rearings across all the groups (Fig. 6E).

Our findings reveal the beneficial role of BHB supplementation in counteracting the detrimental effects of a high-saturated-fat diet on cognitive abilities in mice.

**Discussion**

Recent research has unveiled compelling evidence supporting the effectiveness of nutritional interventions rooted in KD, ketogenic formulas, or BHB supplementation in delaying cognitive loss associated with neurodegenerative disease and enhancing memory performance in individuals with diabetes and healthy aged subjects [7]. There is a noteworthy surge in the popularity of high-fat, low-carbohydrate diets as a strategy for body weight management and obesity treatment [25]. However, to the best of our knowledge, more specific studies are needed to explore the impact of KBs on cognitive damage mediated by nutrients such as saturated fatty acids. In the present study, we demonstrate that intragastric administration of BHB successfully counteracts the memory and learning impairments induced by a SFAD in a mice experimental model. This effect may be attributed to the observed ability of BHB to prevent the adverse impact of palmitic acid on synaptic transmission, excitability and plasticity, and synaptic levels of GluA1-type AMPAR.

*Differential effects of fatty acids on surface GluA1*

AMPARs mediate fast excitatory neurotransmission within the brain and play a pivotal role in various cognitive functions, including memory and learning abilities [14]. In these processes, the formation of new connections and adjustments in synaptic strength require the reorganization of AMPARs in the PSZ. In mature neurons, most synaptic AMPARs comprise the tetramerization of GluA1/GluA2 dimers (constituting 80% of all synaptic AMPARs). A precisely regulated incorporation of GluA1 homomers, which are CP-AMPARs, initiates Ca2+-sensitive signaling events upon glutamate stimulation, contributing to synaptic potentiation and plasticity. Consequently, alterations in the expression of GluA1 or deregulations of its trafficking towards the PM are linked to cognitive impairments [15]. Our study revealed specific alterations in surface GluA1 levels induced by nutrients. Remarkably, PA significantly impacted surface GluA1 levels in both CTX and HPC neurons at an equivalent dosage, manifesting adverse effects even with short treatments. In contrast, OA and DHA exhibited an increase of GluA1 on neuronal surfaces only with more prolonged expositions. Regarding BHB, like PA, we detected increased surface GluA1 levels in HPC and CTX neurons with brief and more prolonged exposures.

Our findings align with existing literature, demonstrating that ω-3 or ω-3-rich oil supplementation in rodents, compared to ω-6-rich, boosts AMPARs and dendritic spine density in the HPC, and LTP during pregnancy and lactation [26–28], suggesting enhanced AMPARs trafficking toward the PM. Conversely, ω-3 deficiency in pups reduces GluA1 in HPC synaptosomes and CA1-HPC LTP [29]. Olive oil, rich in OA, does not impact total or phosphorylated GluA1 levels in the HPC [30], but these observations do not always align with surface GluA1 amount. Given that DHA mitigated some detrimental effects of PA on dendritic length, arborization, and synaptic spines [17,18], and considering the similarities between DHA and OA in the modulation of surface GluA1 depicted in our study, further research into the potential benefits of OA and DHA in PA-induced loss could be of significant interest. Furthermore, we believe that enhancing surface GluA1 mediated by OA or DHA might contribute to the positive effects of PUFAs/MUFAs-enriched diets, such as the Mediterranean diet, on cognitive preservation in the context of metabolic and neurodegenerative diseases.

To our knowledge, the influence of BHB supplementation on the total, surface, or synaptic levels of GluA1 had yet to be evaluated before our study. It has only been described that KD-mediated improvement in short-term memory in young rodents led to increased GluA1 levels in the HPC, with no changes in GluA2 [31]. At the same time, in

adults, KD reduced the expression of GluA1, GluA2, and GluA4-coding genes, yet the impact on cognition was not assessed by [32]. Here, we depicted that BHB treatment increased surface GluA1 levels in cultured neurons without affecting synaptic incorporation. Moreover, the absence of changes in synaptic GluA1 levels was supported by mEPSC recordings. Overall, these results indicated that the rise in surface GluA1 induced by BHB might be confined to the perisynaptic zone—a subset of CP-AMPARs that could be swiftly and transiently mobilized to synapses under specific conditions, controlling the reversibility of both synaptic and spine modifications [22,33]. Moreover, our findings revealed that BHB treatment, particularly at 1 and 2 mM, effectively countered PA-mediated synaptic delivery of GluA1.

Regarding PA, other authors demonstrated that, at 100 mM, there is a reduced AMPA sensitivity in primary cortical neurons, with no observable changes with NMDA [18], suggesting a specific decrease in AMPARs synaptic levels induced by this saturated fat. Nevertheless, the particular impact of PA on the surface or synaptic levels of GluA1 has yet to be investigated thus far. Prior investigations have solely examined its effects in combination with insulin, revealing that the co-treatment heightened GluA1 palmitoylation, concurrently leading to downregulating its recruitment at the PM [19]. Our study demonstrated that PA *per se* was sufficient to downregulate both surface and synaptic levels of GluA1, resulting in a decrease in AMPARs-mediated currents, as evidenced by mEPSC recordings. Considering that the absence of changes in the kinetic parameters implied an unchanged subtype composition of AMPARs, we cannot entirely rule out the possibility that PA might affect other GluA subtypes. Our findings indicate that the reduction in synaptic GluA1 levels exerts a detrimental influence on plasticity, a harmful impact effectively mitigated by concurrent administration of BHB.

*BHB and PA impact on synaptic plasticity*

Similar to AMPARs, the mechanisms underlying how BHB regulates synaptic plasticity still need to be fully understood. While in young or healthy animals, a KD decreased or unaffected LTP, in a mouse model of AD, BHB-mediated improvements in cognition were associated with an increase in LTP [34,35]. Similarly, treating HPC slices with BHB effectively prevented injury-mediated impartment of LTP, while BHB *per se* at 1 or 2 mM did not induce any alterations [36–38]. The current study observed that BHB alone at 2 mM did not significantly alter excitability and synaptic plasticity, as evidenced by input/output curves and LTP recordings. However, BHB demonstrated the capacity to prevent PA-mediated impairments in both paradigms. Under the combined treatment with PA and BHB, neurons exhibited heightened excitability, firing more action

potentials, and sustained synaptic transmission, maintaining connectivity, than with PA alone. Those effects may be attributed to the enhanced presence of AMPARs in the parasynaptic area.

The negative impact of PA on synaptic plasticity has been previously assessed with consistent findings. In HPC slices, whether co-administered with insulin (at 200 mM) [19] or independently at lower concentration (150 μM) [39], PA led to a reduction in LTP without affecting NMDA-mediated long-term depression (LTD). These outcomes align with our results, where we observed a reduction in the AMPA/NMDA ratio in response to PA, indicating that its effects were primarily mediated by a deregulation of AMPARs, rather than NMDARs. Furthermore, the lack of alterations in the PPR and the frequency of the mEPSC, both metrics associated with the probability of vesicular release, supports the assumption that PA and BHB effects were exclusively post-synaptic. These findings indicate that BHB *per se* does not produce substantial changes in excitability or plasticity but might exert a beneficial impact in response to harmful stimuli, such as saturated fats or SFAD.

*BHB levels in the brain*

Though comprising only 2% of body mass, the brain consumes 25% of the body's glucose. 85% of this energy mainly supports glutamate-mediated excitatory synaptic transmission [40]. Nevertheless, during low glucose periods, such as prolonged fasting or low-carbohydrate diet consumption, neurons can utilize BHB as an alternative energy source [41]. While in SD blood, BHB levels range from 0.2 to 2 mM [23], KD elevates BHB levels (0.5-3 mM in blood, 3-5 mM in cerebrospinal fluid) [42,43]. BHB levels in the brain can be assessed using animal models; nevertheless, the considerable variability observed among studies underscores the challenges in determining absolute BHB levels in brain tissue [44–46], underlining the importance of analyzing relative changes. Based on previous studies by [44], we decided to perform a single administration of 100 mg/kg/day BHB in mice. In our study, we observed that intragastric administration efficacy reached BHB levels in the HPC, manifesting as a 2-fold increase in values at 4 hours, comparable to the rise observed in animals fed an SFAD. However, the SFAD *per se*, constituting 49% of calories from saturated fat, failed to raise brain BHB levels compared to a SD, contrasting with previous observations where HFD or KD were associated with increased BHB brain levels [41]. This suggests that the particular response might depend on experimental conditions and diet-specific composition.

*BHB influence on food intake and body weight*

The consumption of ketone esters (often BHB linked to an ester molecule) has been associated with a decrease in energy intake and an increase in energy expenditure (EE), particularly in the presence of high carbohydrate availability, contributing to a slight enhancement in weight loss [47]. In our study, the administration of BHB exhibited no discernible effects on food or energy intake. However, among male mice on a SFDA supplemented with BHB, there was a noteworthy reduction in body weight. This effect was absent in females, who did not exhibit a more significant increase in body weight over the 7-week SFAD period compared to the SD, a finding consistent with the recognized resistance of adult females to diet-induced obesity compared to males [7]. Furthermore, the heightened locomotor activity observed in SFAD-fed mice supplemented with BHB, as revealed in OFT, might increase EE, partially explaining reduced body weight gain in males. Collectively, our data indicate that, despite an increased calorie intake from SFAD, BHB effectively counteracted weight gain in males. Although there is no significant difference in weight gain among females, we observed that SFAD induced cognitive damage in both sexes equally. This underscores that the cognitive impact may precede or surpass the adverse metabolic effects of nutrition, a phenomenon that can be successfully prevented through BHB administration.

*BHB impact on SFAD-mediated cognitive impairment*

The exposure to certain types of obesogenic dietary components, like saturated fatty acids, contributes to cognitive decline [7]. While an excess of dietary fat can negatively impact cognition at any age, particular life stages appear to be especially sensitive to such effects, such as adolescence and elderly stages. Among fats, even for a short consumption period, saturated fats showed deleterious effects on memory compared to isocaloric standard diets at any life stage [16,48,49]. As expected, the consumption of a SFAD (49 kcal from fat) in 5-week-old mice over 2 months successfully induced memory and learning impairments, as evidenced by NORT and OLT results. Our findings revealed that intragastric BHB administration effectively prevents SFAD-induced harmful cognition effects. By *in vitro* results, we did not observe a sustained enhancement in spatial learning and long-term memory performance with BHB under a SD, only an effect in short-term memory. These results align perfectly with previous findings in healthy animals supplemented with BHB or fed a KD, where improvements were observed in short-term memory. At the same time, no changes were reported in the long-term [31,34].

Furthermore, the increased distance traveled by SFAD-fed mice administered with BHB, as observed in OLT, suggested heightened exploration behavior and reduced anxiety. Previous research established associations between BHB administration or KBs supplementation and decreased anxiety in animal models of stress and epilepsy [50,51], as well as increased exploration activity in models of AD [52].

An overall reduction in glutamate receptors, like GluA1, post-synaptic markers, and neuroplasticity-related factors, including brain-derived neurotrophic factor (BDNF), have been consistently associated with plasticity and cognitive impairments mediated by mixed and saturated HFD in animal models [7]. In our experimental conditions, we did not observe any significant changes in the total amount of GluA1 (or its phosphorylation at S845), GluA2, GluN2A, or PSD95 in the HPC across any of the situations. Considering studies with comparable percentages of saturated fats and exposure times, previous research has only reported decreased GluN2A and GluN2B levels following an 8-week diet based on saturated oil-enriched foods [49]. Changes in the total levels of synaptic proteins were observed mainly with longer exposure times or higher percentages of saturated fats [7]. Likewise, a reduction in phosphorylated GluA1 at S845 was documented with a 60% SFAD [19]. However, phosphorylation at this residue constitutes only 0.1% of total GluA1 [24], making establishing a direct association with synaptic GluA1 levels challenging. These findings suggested that cognitive impairments, as mediated by SFAD, or improvements, such as those induced by BHB administration, do not necessarily correlate with adjustments in the total or phosphorylated levels of GluA1.

Additionally, we cannot rule out that other molecular mechanisms may have substantially influenced cognition in response to BHB treatment. *In vitro,* BHB enhanced oxygen consumption, ATP production, mitochondrial respiration, and BNDF production in cortical neurons [53], which plays a vital role in synaptic plasticity and GluA1 translation [54]. *In vivo,* the effects of KD and BHB in ameliorating cognitive decay in AD mouse models are associated with decreased microgliosis, inflammation, and oxidative stress [34,55,56]. All of these hallmarks have also been linked with SFAD-mediated HPC damage [7], suggesting that BHB can reduce these alterations, mitigating cognitive impairments.

In summary, our findings demonstrate that BHB effectively prevents the adverse effects of PA on synaptic GluA1, excitability, and synaptic plasticity, contributing to counteract SFAD-induced cognitive decline. Furthermore, our results provide a potential explanation for the cognitive benefits induced by intermittent fasting [57]. Despite the

predominant release of PA from adipose tissue under fasting conditions, the counteracting effect of BHB production by the liver might be neutralizing the potential harmful effects associated with enhanced PA levels in the brain. Considering that KD or fasting, both conditions elevating blood and brain levels of BHB, often face challenges in long-term adherence [58]**,** we propose that BHB supplementation may yield more satisfactory outcomes to prevent cognitive impairments linked to metabolic diseases.

## Materials and methods

### *Animals and study design*

All animal procedures were performed in agreement with European guidelines (2010/63/EU) and received approval from the Universidad de Barcelona Local Ethical Committee (#222/18). Likewise, animal procedures performed at the Albert Einstein College of Medicine were approved by the Institutional Animal Care and Use Committee (IACUC) in accordance with the National Institutes of Health guidelines. C57BL/6J mice were housed in a controlled environment with a 12-hour light-12-hour dark cycle (lights on at 8 a.m. and off at 8 p.m.), maintaining consistent temperature and humidity. At the age of 5 weeks, the mice were randomly divided into two groups: one group was fed an SD (10% of kcal from fat, 70% from carbohydrates, and 20% from protein; D12450J, Research Diets), while the other group received a SFAD (49% of kcal from fat, 31% from carbohydrates, and 20% from protein; D19121204, Research Diets). Moreover, each group was subdivided into two subgroups: one received intragastrical administration of BHB (H6501, Sigma; 100 mg/kg/day), and the other received an equivalent volume of the vehicle (water). Throughout the study, animals had unrestricted access to food and water. After 7 weeks, the behavior tests were conducted, and mice were euthanized by decapitation 3 days later. Aliquots of serum and tissue samples were collected and stored immediately at -80ºC for subsequent analysis.

### *Primary neuronal cultures*

Primary cortical or hippocampal neurons were derived from mouse E16 embryos and obtained as described previously by [59]. Neurons were cultured and maintained in Neurobasal medium (21103049; Gibco), supplemented with B27 (17504044; Gibco), glutaMAX (35050061; Gibco), and antibiotics. For biochemical assays, cells were seeded at 300,000 cells/mL were in plates coated with poly-D-lysine (0.05 mg/ml; P7886, Sigma-Aldrich). For immunochemistry studies, cortical neurons were seeded at

180,000 cortical cells/mL and hippocampal neurons at 150,000 cells/mL on coverslips-containing plates previously coated with poly-D-lysine (0.1 mg/mL). Cultured neurons were maintained for a period of 2 weeks under controlled conditions at 37$^{o}$C, 5% $CO_2$, and a humidity level of 95%. Every 3-4 days, one-fifth of the medium was replaced with fresh medium.

***Cellular treatments***

OA (O7501, Sigma), PA (P9767, Sigma), and DHA (D8768, Sigma) were prepared to achieve a stock concentration of 3 mM. The fatty acids were dissolved in a defatted BSA solution (0.1 g/mL in 0.9% NaCl; 126575; Millipore), following a method described previously [60]. Additionally, β-hydroxybutyrate (H6501, Sigma) was prepared to obtain a stock concentration of 250 mM and dissolved in water. Cultured neurons were treated at 13-14 days *in vitro* (DIV), with the specific final concentrations as indicated in the results section.

***Immunoblotting***

Protein extract from cultured cells was collected in lysis buffer (20 mM Tris pH 7.5, 5 mM EDTA, 150 mM NaCl, 1% NP40) and from hippocampi and cortex, in RIPA buffer (R0268, Sigma-Aldrich), both supplemented with phosphatase and protease inhibitors (A32957 and A32955, Fisher Scientific). Protein solubilization was achieved through gentle agitation at 4ºC for 30 minutes. Insoluble proteins and unbroken cells were removed by centrifugation at 12,000 rpm for 10 minutes at 4ºC. All protein samples were diluted with loading bu er (containing Tris 1M, 20% SDS, 30% glycerol, and bromophenol) and heated at 95ºC for 5 min. Proteins were separated via 4-15% SDS-PAGE electrophoresis and transferred to a PVDF membrane (IPVH 00010, Millipore). Membranes were immersed in blocking solution (5% nonfat milk in 0.1 % Tween 20 in 1X TBS; TBS: 20 mM Tris, 137 mM NaCl, and 3.9 mM HCl) and incubated overnight with the appropriate antibody at four ºC. Specifically, mouse anti-β-actin (1:5,000; ma1-91399), and anti-GluN2A (1:1,000; 480031) was from ThermoFisher. Mouse anti–β-tubulin (1:2,000; T5201) was purchased from Sigma. Rabbit GluA1 (1:1,000; PC246) was from Millipore. Rabbit PSD95 (1:1,1000; ab18258) and phosphor-GluA1 S845 (ab109464) were from Abcam. Following washing, the membranes were incubated with horseradish peroxidase-tagged secondary anti-mouse or anti-rabbit (1:10,000; 115-035-003 and 111-035-144; Jackson) antibodies in TBS-T (for 1 h at room temperature).

Blots were developed using Luminata Forte (Millipore WBLUF0500) and analyzed with the Syngene Gbox system, with quantification performed using ImageJ software.

***Immunostaining***

Immunostaining of proteins was conducted on fixed cells using 4% (wt/vol) paraformaldehyde (252549, Sigma-Aldrich) as previously described [61]. For surface proteins, non-permeabilized cells were directly blocked with goat serum (g-9023, Sigma-Aldrich), followed by the appropriate primary antibody incubation. In contrast, cells were permeabilized for internal proteins using 0.1% Triton X-100 (vol/vol) before blocking and subsequent incubation with the primary antibody. The primary antibodies used were mouse anti-GluA1 (1:300; ab174785) and rabbit anti-PSD95 (1:30; ab18258), obtained from Abcam. Subsequent incubation with the appropriate Alexa Fluor–conjugated secondary antibody was performed, using anti-rabbit Alexa488 (1:300; A11008) and anti-mouse Alexa568 (1:150; A11011), both purchased from Invitrogen. A brief 5-minute incubation with Hoechst solution (1 µg/mL; 14530, Sigma-Aldrich) was performed to visualize cellular nuclei. Finally, coverslips were mounted using Fluoromount Aqueous Mounting Medium (F4680; Sigma-Aldrich).

***Image acquisition and analysis***

Confocal imaging was conducted on fixed cortical neurons using the Leica DMi8 confocal laser-scanning microscope with a ×63 1.4 NA oil objective. Approximately 18 image stacks, each separated by a 0.5-µm distance, were taken per each imaged cell using identical settings. All subsequent quantifications were performed on reconstructed 3D images using Imaris 9.2 software (Bitplane). Cells were cultured, stained, and imaged simultaneously using identical settings for quantification. To quantify surface GluA1 levels, isolated primary dendrites, representing the initial branches extending from the cell soma, were selected. Axons were identified and excluded based on morphological criteria, including their thickness and relative position to the nucleus. Then, a random region of interest (ROI) measuring 15 µm × 5 µm was chosen, and the integrated intensity within this ROI was measured using the Spot tool in Imaris. To quantify synaptic GluA1 levels, the intensity of GluA1 staining within the 3D ROI defined by PSD95 protein (used as a synaptic marker) was quantified using the Surface tool in Imaris. The same threshold values were applied across all samples to ensure uniformity and accuracy.

***Miniature excitatory synaptic current***

Miniature excitatory synaptic currents (mEPSCs) were conducted in cultured cortical neurons as described previously [62]. Coverslips were mounted in a recording chamber placed on the stage of an inverted microscope (Olympus IX50). Whole–cell patch–clamp currents were recorded using an Axopatch 200B amplifier–Digidata1440A Series interface board with pClamp10 software (Molecular Devices Corporation). Recordings were conducted at room temperature (25-26$^{o}$C). The extracellular solution used for bathing the cells contained the following (in mM): 140 NaCl, 3.5 KCl, 10 HEPES, 20 glucose, 1.8 $CaCl_2$, and 0.8 $MgCl_2$ (pH 7.4 adjusted with NaOH). To isolate AMPAR-mediated mEPSCs, specific blockers were added to the extracellular solution: 1 µM tetrodotoxin (TTX; ab120054 Abcam) to inhibit evoked synaptic transmission, 50 µM D-(-)-2-amino-5-phosphonopentanoic acid (D-AP5; ab120003 Abcam) to block NMDA receptors and 100 µM picrotoxin (PTX; P1675 Sigma-Aldrich) to block $GABA_A$ receptors. Series resistance (Rs) was typically 17.71 ± 0.92 MΩ and was controlled at the experiment's beginning and end. Cells exhibiting a change in Rs greater than 20% were excluded from the analysis. Moreover, mEPSCs were filtered at 2 KHz and digitized at 5 KHz. Events were detected using an amplitude threshold of 5 pA. Only events with monotonic fast rise and uncontaminated decay were included for the amplitude. EPSCs were analyzed with IGOR Pro 6.06 (Wavemetrics) using NeuroMatic 2.03 [63].

**Field excitatory postsynaptic potentials**

To prepare slices, the hippocampi of 1-month-old male mice were dissected and sliced transversally using a vibratome (model VT 1200S; Leica Microsystems) with a thickness of 300 µm. Then, the slices were incubated with a 1:1 proportion of sucrose solution (2.5 mM KCl, 1 mM $CaCl_2$, 4 mM $MgSO_4$, 4 mM $MgCl_2$, 1.6 mM $NaH_2PO_4$, 26 mM $NaHCO_3$, 20 mM glucose, and 215 mM sucrose), and extracellular artificial cerebrospinal fluid (aCSF) solution (124 mM NaCl, 2.5 mM KCl, 2.5 mM $CaCl_2$, 1.3 mM $MgSO_4$, 1 mM $NaH_2PO_4$, 26 mM $NaHCO_3$ and 10 mM glucose) for 20 minutes at 37$^{o}$C oxygenated with a 95% $O_2$/5% $CO_2$ mixture (carbogen). Afterward, a second incubation for 10 minutes was performed, and a last incubation with only a CSF solution for an additional 20 minutes.

fEPSPs were recorded from CA1 pyramidal neurons in the stratum radiatum while stimulating Schaffer collateral (SC) fibers to evoke synaptic responses in dorsal hippocampal slices. Before any recording, the slices were incubated at room temperature for two hours with their respective treatments. For the recordings, glass

pipettes-containing electrodes were employed, with a distance of 100 µm between them. The stimulating electrode was filled with artificial cerebrospinal fluid (CSF), while the recording electrode was filled with NaCl. During the recordings, the slices were placed in an immersion chamber continuously perfused with aCSF, carbogen, and 50 µM PTX at a 2 mL/min rate. The total volume of fluid recirculating through the chamber was 200 mL. Temperature was constantly monitored and maintained at 28 ± 1$^{o}$C. Long-term potentiation (LTP) was induced using a high-frequency stimulation (HFS) protocol consisting of two trains of bursts, each composed of 100 pulses at 100 Hz, with a 10-second interval between them. Data was acquired using an amplifier (model MultiClamp 700A, Molecular Devices). Subsequent data analysis involving the measurement of slope and amplitude was performed using IgorPro software (WaveMetrics). To assess evoked synaptic responses, stimulus intensities were incrementally increased to generate input/output (I/O) curves ranging from 10 to 90 volts. The paired-pulse ratio (PPR) was calculated as the ratio between the slopes or amplitudes of the second response and the first stimulus, with a 10-millisecond interval between them.

Once the voltage clamp seal was achieved, the membrane potential was held at -70 mV. Subsequently, using an extracellular electrode, Schaffer collaterals were stimulated to evoke AMPA-mediated EPSCs in the recorded neuron. After 5-10 minutes, the neuron was depolarized to +30 mV to register NMDA-mediated EPSCs for another 5-10 minutes.
The AMPA/NMDA ratio was obtained by dividing the amplitude of AMPA-mediated EPSCs' amplitude by NMDA-mediated EPSCs' amplitude. Previously, electronic subtraction was performed to remove any residual AMPA current in the recordings conducted at +30 mV. This step was necessary since an AMPA receptor antagonist was not employed to record NMDA-mediated EPSCs.

***BHB determination***

According to the manufacturer's protocol, β-hydroxybutyrate levels were measured using a BHB Assay kit (MAK041, Sigma). This assay measures BHB concentration using a coupled enzyme reaction that produces a colorimetric product at 450 nm. The amount of BHB present was then normalized by the tissue weight.

***Behavior tests***

## *Novel object recognition test (NORT)*

NORT was performed in a 90$^{o}$, two-arm, 25 cm-long, and 20 cm-high maze, as described previously by [64]. Before the test, mice were individually submitted to a 3-day habituation period in the maze, 10 minutes daily. On day 4, they were allowed to explore the maze during a 10-minute acquisition trial (habituation phase), examining two identical novel objects (O1 and O1') placed at the end of each arm. 2 hours later, short-term memory was evaluated with another 10-minute retention trial, where one of the two identical objects was replaced by a novel one (TO). 24 hours later, long-term memory was tested again, using a new object (TN) and one used in the previous trial (TO). The exploration time of the novel object (TN) and the exploration time of the old object (TO) were quantified by visualizing video recordings of each trial session. Object exploration was defined as the mouse's nose touching the object or pointing it toward the object at a distance ≤ 2cm. The cognitive performance was analyzed using the discrimination index (DI) calculated as (TN-TO)/(TN+TO).

***Object location test (OLT)***

HPC-dependent spatial learning was evaluated by OLT using a box (50 x 50 x 25 cm) with three white and one black walls. The box remained empty the first day, allowing mice to acclimate for 10 minutes. The following day, two identical 10-cm-high objects were positioned equidistant from each other and the black wall for 10 minutes. On the last day, one of the objects was relocated in front of the opposite white wall to test spatial memory, quantified as with NORT.

***Open field test (OFT)***

OFT was used to analyze locomotor activity and anxiety-related behaviors (10.1016/j.exger.2016.03.014). In this case, the box (50 x 50 x 25 cm) was divided into central and peripheral zones to facilitate the analysis of the distance traveled. Mice were positioned either at the center or at one of the corners of the open field. After 5 minutes of exploration time, the distance traveled and the number of rearings were analyzed.

***Statistical analysis***

All results are shown as the mean ± standard error (SEM) or standard deviation (SD). Statistical analyses were conducted using the GraphPad Prism 9.0 Sofware. According to the normality test (Shapiro-Wilk test and D'Agostino and Pearson test), Student's t-test, Mann-Whitney U test, or Wilcoxon test were used when comparing only two groups. In cases where multiple groups with different variables were compared, a two-

way analysis of variance (ANOVA) was performed, followed by Bonferroni post hoc tests to assess specific group differences.

## References

## Figure legends

**Figure 1. Nutrient's effects on surface GluA1 levels in primary cortical neurons.** Cortical neurons at 13-14DIV were submitted to PA (200 µM; A), OA (200 µM; B), DHA (200 µM; C), or BHB (5mM; D) treatment, respectively. An equivalent amount of BSA solution was added to control cells when the effects of PA, OA, or DHA were analyzed or water, in the case of BHB. 2 and 24 hours later, neurons were fixed and processed by immunocytochemistry using an anti-GluA1 antibody against the N-terminal domain (extracellular; green stain). Representative images of dendrites are shown (see Supplemental Figure 1 for complete images). In each condition, we analyzed 45 neurons and 2 dendrites per neuron from three independent experiments performed by biological duplicates. The results in the graphs are the integrated intensity of surface GluA1 normalized by the control given as the mean ± SEM. (A) Left, control 2h (BSA; 1.00 ± 0.06, n = 79), and PA 2h (0.70 ± 0.07, n = 82); right, control 24h (BSA; 1.00 ± 0.04, n = 77), and PA 24h (0.60 ± 0.03, n = 72). (B) Left, control 2h (BSA; 1.00 ± 0.04, n = 84), and OA 2h (1.08 ± 0.04, n = 86); left, control 24h (BSA; 1.00 ± 0.04, n = 80), and OA 24h (1.19 ± 0.06, n = 60). (C) Left, control 2h (BSA; 1.00 ± 0.03, n = 93), and DHA 2h (1.08 ± 0.04, n = 114); right, control 24h (BSA; 1.00 ± 0.03, n = 100), and DHA 24h (1.16 ± 0.05, n = 99). (D) Left, control 2h (1.00 ± 0.04, n = 98), and BHB 2h (1.22 ± 0.04, n = 86); right, control 24h (1.00 ± 0.04, n = 95), and BHB 24h (1.30 ± 0.05, n = 93). **, $P < 0.05$; ***, $P < 0.001$; ****, $P < 0.0001$. Student t-test. Scale bar = 10 µm.

**Figure 2. Palmitate and BHB effects on mEPSC in cortical neurons.** Cultured cortical neurons (14-15 DIV) were treated with PA (200µM) or BHB (5mM) for 24h. An equivalent amount of vehicle (BSA solution) was added to control neurons and BHB-treated ones to compare all the conditions properly. A) Representative whole-cell recordings of AMPAR-mediated mEPSCs of 15 seconds duration. Inset magnifications correspond to 1.5 seconds. Membrane potential was held at -70 mV. B) Examples of averaged mEPSCs (bold lines) from 11-, 7- and 5-minutes of time (control, PA, and BHB, respectively) of the recordings shown in A. Control neurons exhibited a mean mEPSCs amplitude of –18 pA (average of 2815 miniature events); PA-treated ones (central traces), –12.1 pA (1967 events); and BHB-treated ones, –18.38 pA (1098 events). One hundred random individual mEPSCs events for the three recordings are

shown in grey. C) AMPAR mEPSCs amplitude was decreased in PA-treated cells compared with control neurons (-18.07 ± 1.20 pA, n=26; -13.28 ± 1.20 pA, n=21; and -17.25 ± 1.27 pA, n=19 for control, PA, and BHB-treated neurons respectively respectively). D) Cumulative probability distribution of mEPSCs amplitude showing a leftward shift in amplitude for events of PA-treated neurons. Continuous lines represent the average for control (black line; n=26 neurons; an average of 1104 events/neuron) and PA (red line; n=21; 768 events/neuron). Discontinuous lines denote the SEM. E) AMPAR mEPSCs frequency was not altered with PA nor with BHB (5.04 ± 0.92 Hz; 2.82 ± 0.44 Hz; and 3.32 ± 0.53 Hz; for control, PA, and BHB, respectively). F) AMPAR mEPSCs rise time was not altered with PA nor with BHB (1.96 ± 0.05 ms; 1.90 ± 0.06 ms; and 1.93 ± 0.04 ms for control, PA, and BHB, respectively). G) AMPAR mEPSCs τ-weighted was not altered either with palmitate nor with BHB (3.94 ± 0.21 ms; 4.35 ± 0.35 ms; and 4.00 ± 0.21 ms; for control, PA, and BHB, respectively). **, $P < 0.01$. Mann-Whitney test by comparing each condition with the control.

**Figure 3. Short-term effects of palmitate and BHB on synaptic GluA1 levels in hippocampal neurons.** Cultured hippocampal neurons (14-15 DIV) were treated with PA (200 µM) and/or BHB (1,2 or 5 mM). An equivalent amount of vehicle (BSA solution) was added to control neurons and BHB-treated ones to properly compare all the conditions. 2 hours later, in non-permeabilized cells, GluA1 was detected by immunostaining. Then, cells were permeabilized, and a subsequent immunostaining was used to identify the synaptic marker PSD95. To determine synaptic GluA1 levels, the integrated intensity of GluA1 staining within the PSD95-defined ROI was quantified. Results in the graphs are given as mean ± SEM of 60 dendrites from two independent experiments performed by biological duplicates. Control (BSA; 1.00 ± 0.09, n=54), PA (0.44 ± 0.06, n=56), 1 mM BHB (0.89 ± 0.05, n=53), 2 mM BHB (1.02 ± 0.04, n=65), 5 mM BHB (1.34 ± 0.07, n=53), PA + 1 mM BHB (0.92 ± 0.05, n=52), PA + 2 mM BHB (0.93 ± 0.05, n=45), and PA + 5 mM BHB (0.68 ± 0.06, n=47). Scale bar = 40 µm; scale bar of inset magnifications = 10 µm. ****, $P < 0.0001$. One-way ANOVA followed by the Bonferroni test.

**Figure 4. BHB reverses palmitate-induced impairment in electrophysiological input/output currents and LTP in hippocampal slices**. A) Superimposed fEPSP traces induced by a series of stimulating pulses with an increase of 10 mV applied to the SC fiber. B) Input/output curves plotted with the increased fEPSP slopes corresponding to the enhanced stimulating intensities. Results in the graphs are the mean ± SD of n = 10-17 slices per condition taken from 4 male mice (P26 ± 5). Two-

way ANOVA was followed by the Bonferroni. C) Time course of normalized slope of AMPAR-mediated EPSCs from baseline and after induction of LTP. Results in the graphs are the mean ± SD of n = 3-4 slices per condition taken from 3-4 male mice (P27-34). One-way ANOVA was followed by the Bonferroni. D) Representative traces of the baseline (thin lines) and the last 5 minutes of the time course after LTP induction (thick lines). E) Targeted patch-clamp recordings from CA1 pyramidal cells at stratum radiatum while stimulating SC fibers. H-F) Representative traces of AMPA and NMDA receptor-mediated postsynaptic currents were recorded at -70 and +30 mV, respectively. G) Results in the graphs showing the effect of the different treatments on the AMPA/NMDA ratio are represented as mean ± SEM, n=5-6 cells from 3-5 male mice (P26 ± 5) per condition. Control (3.73 ± 0.59, n=6), vehicle (4.16 ± 0.74, n=5), PA (2.25 ± 0.31, n=6), and BHB (4.40 ± 0.66, n=6). Student t-test by comparing each condition with the control. *, P < 0.05; **, P < 0.01; and ****, P < 0.0001.

**Figure 5. Effect of BHB administration in bodyweight gain mediated by SFAD.** A) Animals' study design. 5-weeks old-mice were divided into 4 groups: SD (10% of kcal from fatty acids) + vehicle (equal amount of water), SD + BHB administration (100mg/kg/day), SFAD (49% of kcal from saturated fatty acids) + vehicle, and SFAD + BHB. Animals were maintained for 7 weeks under these feeding conditions and submitted to behavior test 3 days before the sacrifice to obtain blood and tissue samples. B) The BHB levels in HPC. The results in the graphs are the mean ± SD. SD + vehicle (0.16 ± 0.08, n=7), SD + BHB (0.23 ± 0.12, n=8), SFAD + vehicle (0.10 ± 0.04, n=7), and SFAD + BHB (0.26 ± 0.08, n=8). C-D) The animals were weighed weekly. Male and female weight is shown in C and D, respectively. Data are represented as mean ± SD from n=5-7/group. *, P < 0.05; and **, P < 0.01. One-way ANOVA was followed by the Bonferroni.

**Figure 6. Effect of BHB administration in cognitive impairment mediated by SFAD.** A-C) NORT was performed 2h (A) and 24 hours (B) after the habituation phase, respectively. OLT was performed to evaluate spatial memory (C). The results of the discrimination index (DI) in the graphs are the mean ± SD. NORT 2h: SD + vehicle (0.24 ± 0.12, n=11), SD + BHB (0.44 ± 0.28, n=9), SFAD + vehicle (0.02 ± 0.16, n=11), and SFAD + BHB (0.25 ± 0.14, n=11). NORT 24h: SD + vehicle (0.18 ± 0.37, n=11), SD + BHB (0.36 ± 0.21, n=9), SFAD + vehicle (-0.01 ± 0.12, n=11), and SFAD + BHB (0.33 ± 0.14, n=11). OLT: SD + vehicle (0.26 ± 0.03, n=11), SD + BHB (0.19 ± 0.002, n=9), SFAD + vehicle (-0.06 ± 0.05, n=11), and SFAD + BHB (0.26 ± 0.05, n=11). D-E) Locomotor activity and the number of rearings were measured using OFT. Data are

represented as mean ± SD. Locomotor activity: SD + vehicle (1059 ± 154, n=11), SD + BHB (914 ± 109, n=9), SFAD + vehicle (1079 ± 134, n=11), and SFAD + BHB (1274 ± 101, n=11). Rearings: SD + vehicle (26.5 ± 9.2, n=11), SD + BHB (27.4 ± 9.0, n=9), SFAD + vehicle (21.7 ± 5.4, n=11), and SFAD + BHB (28.6 ± 8.8, n=11). **, P < 0.01; and ****, P < 0.0001. One-way ANOVA followed by Bonferroni test.

**Supplemental data**

**Supplemental Figure 1. Complete images of nutrient's effects on surface GluA1 levels in primary cortical neurons.** Cortical neurons at 13-14DIV were submitted to PA (200 µM; A-B), OA (200 µM; C-D), DHA (200 µM; E-F), or BHB (5mM; G-H) treatment for 2 or 24 hours, respectively. Surface GluA1 was detected by IC (green stain) and nuclei by Hoechst staining (in blue). The magnifications of images are shown in Figure 1. Scale bar = 40 µm

**Supplemental Figure 2. Differentiated SH-SY5Y successfully mimics nutrients' effects on surface GluA1 levels. The** SH-SY5H cell line was differentiated to a neuron-like phenotype with retinoic acid (10µM). 6 days later, cells were exposed for 24 hours to PA (200 µM; A), OA (200 µM; B), DHA (200 µM; C), or BHB (5mM; D), respectively. Then, nonpermeabilized cells were fixed and processed, as in Figure 1. Representative images of neurites are shown on the right. In each condition, we analyzed 22-35 neurites from one (DHA) or two (PA, OA, and BHB) independent experiments performed by biological duplicates. Results in left graphs are given as mean ± SEM. (A) Control (BSA; 1.00 ± 0.08, n = 36), and PA (0.71 ± 0.05, n = 36). (B) Control (BSA; 1.00 ± 0.08, n = 36), and OA (1.63 ± 0.09, n = 35). (C) Control (BSA; 1.00 ± 0.10, n = 26), and DHA (1.56 ± 0.12, n = 28). (D) Control (1.00 ± 0.06, n = 44), and BHB (1.62 ± 0.11, n = 40). **, P < 0.05; ***, P < 0.001; ****, P < 0.0001. Student t-test. Scale bar = 25 µm; scale bar of inset magnifications = 5 µm. *p<0.05.

**Supplemental Figure 3. PA decreases, and high-dose BHB increases surface GluA1 levels in hippocampal neurons.** The surface GluA1 levels from the same experiments done in Figure 3 are shown. Results in the graphs are given as mean ± SEM of 60 dendrites from two independent experiments performed by biological duplicates. Control (BSA; 1.00 ± 0.04, n=64), PA (0.59 ± 0.02, n=69),1 mM BHB (0.89 ± 0.05, n=53), 2 mM BHB (1.02 ± 0.04, n=65), and 5 mM BHB (1.34 ± 0.07, n=53). Scale bar = 40 µm; scale bar of inset magnifications = 10 µm. ****, P < 0.0001. One-way ANOVA followed by Bonferroni test.

**Supplemental Figure 4. Effects of BHB, palmitate, and co-treatment of hippocampal slices on paired-pulse ratio.** Average values of PPRs from fEPSP with 100 ms interstimulus interval. Individual values for each condition are displayed as a dot plot. Data are represented as mean ± SEM of n = 10-17 slices from 4 male mice (P26 ± 5) per condition. Representative traces for each condition are shown. PPR slope: control (1.70 ± 0.05, n=17), BHB (1.81 ± 0.06; n=9), vehicle (1.78 ± 0.07, n=12), PA (1.73 ± 0.06, n=17), and PA + BHB (1.74 ± 0.08, n=12). PPR amplitude: control (1.79 ± 0.06, n=18), BHB (1.94 ± 0.06; n=10), vehicle (1.79 ± 0.06, n=12), PA (1.71 ± 0.05, n=17), and PA + BHB (1.78 ± 0.08, n=12). One-way ANOVA followed by Bonferroni test.

**Supplemental Figure 5. BHB hippocampal levels and food intake after BHB administration and SFAD feeding.** A) BHB pharmacokinetic assay. BHB levels were measured in the HPC of mice at 30 minutes, 1 hour, 2 hours, 4 hours, and 24 hours following intragastric administration of BHB (100 mg/kg). Results are represented as mean ± SD from n=2-4/time point. B-C) The food was weighed weekly. Cumulative food intake is shown in g (B) and calorie intake, in kcal (C). Data are represented as mean ± SD from n=9-11/group. **, P < 0.01. One-way ANOVA followed by Bonferroni test.

**Supplemental Figure 6. Synaptic proteins in the hippocampus, locomotor activity, and rearing after BHB administration and SFAD feeding.** The levels of different synaptic proteins were analyzed by Western blot in whole hippocampi. The results in the graphs are the mean ± SD. A) GluA1 whole HPC: SD + vehicle (1.00 ± 0.20, n=8), SD + BHB (0.96 ± 0.23, n=7), SFAD + vehicle (1.02 ± 0.22, n=8), and SFAD + BHB (0.94 ± 0.14, n=8). B) P(S845)-GluA1 whole HPC: SD + vehicle (1.00 ± 0.34, n=8), SD + BHB (1.08 ± 0.38, n=7), SFAD + vehicle (0.66 ± 0.25, n=8), and SFAD + BHB (0.74 ± 0.16, n=8). C) GluA2 whole HPC: SD + vehicle (1.00 ± 0.33, n=8), SD + BHB (1.03 ± 0.40, n=7), SFAD + vehicle (1.07 ± 0.38, n=8), and SFAD + BHB (1.13 ± 0.29, n=8). D) GluN2A whole HPC: SD + vehicle (1.00 ± 0.36, n=8), SD + BHB (0.96 ± 0.20, n=7), SFAD + vehicle (1.00 ± 0.25, n=8), and SFAD + BHB (0.92 ± 0.23, n=8). E) PSD95 whole HPC: SD + vehicle (1.00 ± 0.23, n=8), SD + BHB (1.04 ± 0.21, n=7), SFAD + vehicle (0.99 ± 0.24, n=8), and SFAD + BHB (1.02 ± 0.27, n=8).

## Supplemental materials and methods

### *Cell line and treatment*

SH-SY5Y cells, derived from SH-SY subclone of the parental SK-N-SH human neuroblastoma cell line, were cultured in Dulbecco's Modified Eagle's Medium (DMEM; D5671, Sigma-Aldrich) supplemented with 10% fetal bovine serum (FBS12A, Capricorn Scientific), 1% glutamax (X0551-100, Biowest), 100 U/ mL penicillin and 100 µg/mL streptomycin (P0781, Sigma-Aldrich), and maintained at 37°C in 5% CO2 humidified air. Cell line was tested for mycoplasma contamination using EZ-PCR™ Mycoplasma Detection Kit (20-700-20BI). To induce neuron-like phenotype, cells were seeded at 40,000 cells/mL in collagen-coated coverslips (1:50; 354236, Corning) and cultured in medium supplemented with 10 µM of retinoic acid (R2622, Sigma) diluted in DMSO (1029521011, Merck). Differentiated SH-SY5Y cells were subjected to treatment 6 days after, with the specific final concentrations as indicated in results section.

**Acknowledgements**

This study was supported by the Spanish Ministry of Science and Innovation (MCIN) (PID2020-114953RB-C22 to NC) co-funded by the European Regional Development Fund, the Biomedical Research Centre in Pathophysiology of Obesity and Nutrition (CIBEROBN) (Grant CB06/03/0001 to NC). The work performed at Universitat de Barcelona was supported by Fondo Europeo de Desarrollo Regional (MINECO-FEDER) (PID2022-139016OA-I00 and PDC2022-133441-I00; to C.G-F. and M.P.), and Generalitat de Catalunya (2021 SGR 00357). P.E.C, E.G, and the work performed at the Albert Einstein College of Medicine was supported by NIH grants R01MH116673, R01MH125772, and R01NS113600.

**Author Contributions**

Conceptualization, R.R., R.F. and N.C., Methodology, R.R., R.F., M.M., C.G-F., A.C., and D.S.; Software, R.R., R.F., C.G-F., A.C., and D.S.; Formal Analysis and Data Curation, R.F. and R.R.; Investigation, R.R., R.F., C.G-F., A.C., and D.S; Resources, J. R-A., D.S., P.C., M.P., and N.C.; Writing – Original Draft Preparation, R.F. R.R., and N.C.; Writing – Review & Editing, all the authors; Supervision, R.F., C.G-F., M.P. and N.C.; Funding Acquisition, L.J., J.N., J. R-A., D.S, P.E.C., C.G-F., M.P., and N.C.

**Conflicts of interest**

The authors declare no conflict of interest.

**Bibliography**

1. World Health Organization Dementia: Number of People Affected to Triple in

next 30 Years Available online: http://www.who.int/fr/news-room/detail/07-12-2017-dementia-number-of-people-affected-to-triple-in-next-30-years (accessed on 7 December 2017).

2. Dye, L.; Boyle, N.B.; Champ, C.; Lawton, C. The Relationship between Obesity and Cognitive Health and Decline. *Proc. Nutr. Soc.* **2017**, *76*, 443–454, doi:10.1017/S0029665117002014.

3. Bramorska, A.; Zarzycka, W.; Podolecka, W.; Kuc, K.; Brzezicka, A. Age-Related Cognitive Decline May Be Moderated by Frequency of Specific Food Products Consumption. *Nutrients* **2021**, *13*, doi:10.3390/NU13082504/S1.

4. World Health Organization Obesity and Overweight Available online: https://www.who.int/news-room/fact-sheets/detail/obesity-and-overweight (accessed on 12 September 2022).

5. Singh-Manoux, A.; Dugravot, A.; Shipley, M.; Brunner, E.J.; Elbaz, A.; Sabia, S.; Kivimaki, M. Obesity Trajectories and Risk of Dementia: 28 Years of Follow-up in the Whitehall II Study. *Alzheimers. Dement.* **2018**, *14*, 178–186, doi:10.1016/j.jalz.2017.06.2637.

6. Coppin, G.; Nolan-Poupart, S.; Jones-Gotman, M.; Small, D.M. Working Memory and Reward Association Learning Impairments in Obesity. *Neuropsychologia* **2014**, *65*, 146–155, doi:10.1016/j.neuropsychologia.2014.10.004.

7. Fadó, R.; Molins, A.; Rojas, R.; Casals, N. Feeding the Brain: Effect of Nutrients on Cognition, Synaptic Function, and AMPA Receptors. *Nutrients* **2022**, *14*, doi:10.3390/NU14194137.

8. Baym, C.L.; Khan, N.A.; Monti, J.M.; Raine, L.B.; Drollette, E.S.; Moore, R.D.; Scudder, M.R.; Kramer, A.F.; Hillman, C.H.; Cohen, N.J. Dietary Lipids Are Differentially Associated with Hippocampal-Dependent Relational Memory in Prepubescent Children. *Am. J. Clin. Nutr.* **2014**, *99*, 1026–1033, doi:10.3945/AJCN.113.079624.

9. Okereke, O.I.; Rosner, B.A.; Kim, D.H.; Kang, J.H.; Cook, N.R.; Manson, J.E.; Buring, J.E.; Willett, W.C.; Grodstein, F. Dietary Fat Types and 4-Year Cognitive Change in Community-Dwelling Older Women. *Ann. Neurol.* **2012**, *72*, 124–134, doi:10.1002/ANA.23593.

10. Golomb, B.A.; Bui, A.K. A Fat to Forget: Trans Fat Consumption and Memory. *PLoS One* **2015**, *10*, doi:10.1371/JOURNAL.PONE.0128129.

11. Canhada, S.; Castro, K.; Perry, I.S.; Luft, V.C. Omega-3 Fatty Acids' Supplementation in Alzheimer's Disease: A Systematic Review. *Nutr. Neurosci.* **2018**, *21*, 529–538, doi:10.1080/1028415X.2017.1321813.

12. Vinciguerra, F.; Graziano, M.; Hagnäs, M.; Frittitta, L.; Tumminia, A. Influence of the Mediterranean and Ketogenic Diets on Cognitive Status and Decline: A Narrative Review. *Nutrients* **2020**, *12*, doi:10.3390/nu12041019.

13. Kouvari, M.; D'cunha, N.M.; Travica, N.; Sergi, D.; Zec, M.; Marx, W.; Naumovski, N. Metabolic Syndrome, Cognitive Impairment and the Role of Diet: A Narrative Review. *Nutrients* **2022**, *14*, doi:10.3390/NU14020333.

14. Hanley, J.G. Subunit-Specific Trafficking Mechanisms Regulating the Synaptic Expression of Ca2+-Permeable AMPA Receptors. *Semin. Cell Dev. Biol.* **2014**, *27*, 14–22, doi:10.1016/j.semcdb.2013.12.002.

15. Jurado, S. AMPA Receptor Trafficking in Natural and Pathological Aging. *Front. Mol. Neurosci.* **2018**, *10*, doi:10.3389/FNMOL.2017.00446.

16. Granholm, A.C.; Bimonte-Nelson, H.A.; Moore, A.B.; Nelson, M.E.; Freeman, L.R.; Sambamurti, K. Effects of a Saturated Fat and High Cholesterol Diet on Memory and Hippocampal Morphology in the Middle-Aged Rat. *J. Alzheimer's Dis.* **2008**, *14*, 133–145, doi:10.3233/JAD-2008-14202.

17. McLean, F.H.; Campbell, F.M.; Sergi, D.; Grant, C.; Morris, A.C.; Hay, E.A.; MacKenzie, A.; Mayer, C.D.; Langston, R.F.; Williams, L.M. Early and Reversible Changes to the Hippocampal Proteome in Mice on a High-Fat Diet. *Nutr. Metab.* **2019**, *16*, 1–12, doi:10.1186/s12986-019-0387-y.

18. Loehfelm, A.; Elder, M.K.; Boucsein, A.; Jones, P.P.; Williams, J.M.; Tups, A. Docosahexaenoic Acid Prevents Palmitate-Induced Insulin-Dependent Impairments of Neuronal Health. *FASEB J.* **2020**, *34*, 4635–4652, doi:10.1096/fj.201902517R.

19. Spinelli, M.; Fusco, S.; Mainardi, M.; Scala, F.; Natale, F.; Lapenta, R.; Mattera, A.; Rinaudo, M.; Li Puma, D.D.; Ripoli, C.; et al. Brain Insulin Resistance Impairs Hippocampal Synaptic Plasticity and Memory by Increasing GluA1

Palmitoylation Through. *Nat. Commun.* **2017**, *8*, 1–14, doi:10.1038/s41467-017-02221-9.

20. Page, K.A.; Williamson, A.; Yu, N.; McNay, E.C.; Dzuira, J.; McCrimmon, R.J.; Sherwin, R.S. Medium-Chain Fatty Acids Improve Cognitive Function in Intensively Treated Type 1 Diabetic Patients and Support in Vitro Synaptic Transmission during Acute Hypoglycemia. *Diabetes* **2009**, *58*, 1237–1244, doi:10.2337/db08-1557.

21. Jensen, N.J.; Nilsson, M.; Ingerslev, J.S.; Olsen, D.A.; Fenger, M.; Svart, M.; Møller, N.; Zander, M.; Miskowiak, K.W.; Rungby, J. Effects of β-Hydroxybutyrate on Cognition in Patients with Type 2 Diabetes. *Eur. J. Endocrinol.* **2020**, *182*, 233–242, doi:10.1530/EJE-19-0710.

22. Yang, Y.; Wang, X. Bin; Frerking, M.; Zhou, Q. Delivery of AMPA Receptors to Perisynaptic Sites Precedes the Full Expression of Long-Term Potentiation. *Proc. Natl. Acad. Sci. U. S. A.* **2008**, *105*, 11388–11393, doi:10.1073/PNAS.0802978105.

23. Nehlig, A. Brain Uptake and Metabolism of Ketone Bodies in Animal Models. *Prostaglandins Leukot. Essent. Fat. Acids* **2004**, *70*, 265–275, doi:10.1016/j.plefa.2003.07.006.

24. Hosokawa, T.; Mitsushima, D.; Kaneko, R.; Hayashi, Y. Stoichiometry and Phosphoisotypes of Hippocampal AMPA-Type Glutamate Receptor Phosphorylation. *Neuron* **2015**, *85*, 60–67, doi:10.1016/J.NEURON.2014.11.026.

25. Basolo, A.; Magno, S.; Santini, F.; Ceccarini, G. Ketogenic Diet and Weight Loss: Is There an Effect on Energy Expenditure? *Nutrients* **2022**, *14*, doi:10.3390/NU14091814.

26. Lee, J.; Park, S.; Lee, J.Y.; Yeo, Y.K.; Kim, J.S.; Lim, J. Improved Spatial Learning and Memory by Perilla Diet Is Correlated with Immunoreactivities to Neurofilament and α-Synuclein in Hilus of Dentate Gyrus. *Proteome Sci.* **2012**, *10*, doi:10.1186/1477-5956-10-72.

27. Cansev, M.; Wurtman, R.J.; Sakamoto, T.; Ulus, I.H. Oral Administration of Circulating Precursors for Membrane Phosphatides Can Promote the Synthesis of New Brain Synapses. *Alzheimers. Dement.* **2008**, *4*,

doi:10.1016/J.JALZ.2007.10.005.

28. Kavraal, S.; Oncu, S.K.; Bitiktas, S.; Artis, A.S.; Dolu, N.; Gunes, T.; Suer, C. Maternal Intake of Omega-3 Essential Fatty Acids Improves Long Term Potentiation in the Dentate Gyrus and Morris Water Maze Performance in Rats. *Brain Res.* **2012**, *1482*, 32–39, doi:10.1016/j.brainres.2012.09.002.

29. Aryal, S.; Hussain, S.; Drevon, C.A.; Nagelhus, E.; Hvalby, Ø.; Jensen, V.; Walaas, S.I.; Davanger, S. Omega-3 Fatty Acids Regulate Plasticity in Distinct Hippocampal Glutamatergic Synapses. *Eur. J. Neurosci.* **2019**, *49*, 40–50, doi:10.1111/EJN.14224.

30. Cutuli, D.; de Bartolo, P.; Caporali, P.; Laricchiuta, D.; Foti, F.; Ronci, M.; Rossi, C.; Neri, C.; Spalletta, G.; Caltagirone, C.; et al. N-3 Polyunsaturated Fatty Acids Supplementation Enhances Hippocampal Functionality in Aged Mice. *Front. Aging Neurosci.* **2014**, *6*, 1–53, doi:10.3389/fnagi.2014.00220.

31. Fukushima, A.; Ogura, Y.; Furuta, M.; Kakehashi, C.; Funabashi, T.; Akema, T. Ketogenic Diet Does Not Impair Spatial Ability Controlled by the Hippocampus in Male Rats. *Brain Res.* **2015**, *1622*, 36–42, doi:10.1016/j.brainres.2015.06.016.

32. Hernandez, A.R.; Hernandez, C.M.; Truckenbrod, L.M.; Campos, K.T.; McQuail, J.A.; Bizon, J.L.; Burke, S.N. Age and Ketogenic Diet Have Dissociable Effects on Synapse-Related Gene Expression Between Hippocampal Subregions. *Front. Aging Neurosci.* **2019**, *11*, doi:10.3389/FNAGI.2019.00239.

33. Yang, Y.; Wang, X. Bin; Zhou, Q. Perisynaptic GluR2-Lacking AMPA Receptors Control the Reversibility of Synaptic and Spines Modifications. *Proc. Natl. Acad. Sci. U. S. A.* **2010**, *107*, 11999–12004, doi:10.1073/PNAS.0913004107.

34. Yin, J.X.; Maalouf, M.; Han, P.; Zhao, M.; Gao, M.; Dharshaun, T.; Ryan, C.; Whitelegge, J.; Wu, J.; Eisenberg, D.; et al. Ketones Block Amyloid Entry and Improve Cognition in an Alzheimer's Model. *Neurobiol. Aging* **2016**, *39*, 25–37, doi:10.1016/j.neurobiolaging.2015.11.018.

35. Blaise, J.H.; Ruskin, D.N.; Koranda, J.L.; Masino, S.A. Effects of a Ketogenic Diet on Hippocampal Plasticity in Freely Moving Juvenile Rats. *Physiol. Rep.* **2015**, *3*, 1–8, doi:10.14814/phy2.12411.

36. Maalouf, M.; Rho, J.M. Oxidative Impairment of Hippocampal Long-Term

Potentiation Involves Activation of Protein Phosphatase 2A and Is Prevented by Ketone Bodies. *J. Neurosci. Res.* **2008**, *86*, 3322–3330, doi:10.1002/JNR.21782.

37. Kimura, R.; Ma, L.Y.; Wu, C.; Turner, D.; Shen, J.X.; Ellsworth, K.; Wakui, M.; Maalouf, M.; Wu, J. Acute Exposure to the Mitochondrial Complex I Toxin Rotenone Impairs Synaptic Long-Term Potentiation in Rat Hippocampal Slices. *CNS Neurosci. Ther.* **2012**, *18*, 641–646, doi:10.1111/J.1755-5949.2012.00337.X.

38. Youssef, F.F. Ketone Bodies Attenuate Excitotoxic Cell Injury in the Rat Hippocampal Slice under Conditions of Reduced Glucose Availability. *Neurol. Res.* **2015**, *37*, 211–216, doi:10.1179/1743132814Y.0000000430.

39. Contreras, A.; Del Rio, D.; Martínez, A.; Gil, C.; Morales, L.; Ruiz-Gayo, M.; Del Olmo, N. Inhibition of Hippocampal Long-Term Potentiation by High-Fat Diets: Is It Related to an Effect of Palmitic Acid Involving Glycogen Synthase Kinase-3? *Neuroreport* **2017**, *28*, 354–359, doi:10.1097/WNR.0000000000000774.

40. Harris, J.J.; Jolivet, R.; Attwell, D. Synaptic Energy Use and Supply. *Neuron* **2012**, *75*, 762–777, doi:10.1016/j.neuron.2012.08.019.

41. Jensen, N.J.; Wodschow, H.Z.; Nilsson, M.; Rungby, J. Effects of Ketone Bodies on Brain Metabolism and Function in Neurodegenerative Diseases. *Int. J. Mol. Sci.* **2020**, *21*, 1–17, doi:10.3390/IJMS21228767.

42. Lowder, J.; Fallah, S.; Venditti, C.; Musa-Veloso, K.; Kotlov, V. An Open-Label, Acute Clinical Trial in Adults to Assess Ketone Levels, Gastrointestinal Tolerability, and Sleepiness Following Consumption of (R)-1,3-Butanediol (Avela$^{TM}$). *Front. Physiol.* **2023**, *14*, doi:10.3389/FPHYS.2023.1195702/FULL.

43. Masino, S.A.; Ruskin, D.N.; Freedgood, N.R.; Lindefeldt, M.; Dahlin, M. Differential Ketogenic Diet-Induced Shift in CSF Lipid/Carbohydrate Metabolome of Pediatric Epilepsy Patients with Optimal vs. No Anticonvulsant Response: A Pilot Study. *Nutr. Metab. (Lond).* **2021**, *18*, doi:10.1186/S12986-020-00524-1.

44. Hu, E.; Du, H.; Zhu, X.; Wang, L.; Shang, S.; Wu, X.; Lu, H.; Lu, X. Beta-Hydroxybutyrate Promotes the Expression of BDNF in Hippocampal Neurons under Adequate Glucose Supply. *Neuroscience* **2018**, *386*, 315–325, doi:10.1016/j.neuroscience.2018.06.036.

45. Son, H.; Baek, J.H.; Kang, J.S.; Jung, S.; Chung, H.J.; Kim, H.J. Acutely Increased β-Hydroxybutyrate Plays a Role in the Prefrontal Cortex to Escape Stressful Conditions during the Acute Stress Response. *Biochem. Biophys. Res. Commun.* **2021**, *554*, 19–24, doi:10.1016/J.BBRC.2021.03.062.

46. Zhang, J.; Cao, Q.; Li, S.; Lu, X.; Zhao, Y.; Guan, J.S.; Chen, J.C.; Wu, Q.; Chen, G.Q. 3-Hydroxybutyrate Methyl Ester as a Potential Drug against Alzheimer's Disease via Mitochondria Protection Mechanism. *Biomaterials* **2013**, *34*, 7552–7562, doi:10.1016/J.BIOMATERIALS.2013.06.043.

47. Fernández-Verdejo, R.; Mey, J.T.; Ravussin, E. Effects of Ketone Bodies on Energy Expenditure, Substrate Utilization, and Energy Intake in Humans. *J. Lipid Res.* **2023**, *64*, doi:10.1016/J.JLR.2023.100442.

48. Beilharz, J.E.; Kaakoush, N.O.; Maniam, J.; Morris, M.J. The Effect of Short-Term Exposure to Energy-Matched Diets Enriched in Fat or Sugar on Memory, Gut Microbiota and Markers of Brain Inflammation and Plasticity. *Brain. Behav. Immun.* **2016**, *57*, 304–313, doi:10.1016/j.bbi.2016.07.151.

49. Fernández-Felipe, J.; Merino, B.; Sanz-Martos, A.B.; Plaza, A.; Contreras, A.; Naranjo, V.; Morales, L.; Chowen, J.A.; Cano, V.; Ruiz-Gayo, M.; et al. Saturated and Unsaturated Fat Diets Impair Hippocampal Glutamatergic Transmission in Adolescent Mice. *Psychoneuroendocrinology* **2021**, *133*, doi:10.1016/J.PSYNEUEN.2021.105429.

50. Yamanashi, T.; Iwata, M.; Shibushita, M.; Tsunetomi, K.; Nagata, M.; Kajitani, N.; Miura, A.; Matsuo, R.; Nishiguchi, T.; Kato, T.A.; et al. Beta-Hydroxybutyrate, an Endogenous NLRP3 Inflammasome Inhibitor, Attenuates Anxiety-Related Behavior in a Rodent Post-Traumatic Stress Disorder Model. *Sci. Rep.* **2020**, *10*, doi:10.1038/S41598-020-78410-2.

51. Rauch, E.; Ari, C.; Kovács, Z. Dose-Dependent Beneficial Effect of Ketone Supplement-Evoked Ketosis on Anxiety Level in Female WAG/Rij Rats: Sometimes Less Is More. *Nutrients* **2023**, *15*, doi:10.3390/NU15204412.

52. Pawlosky, R.J.; Kashiwaya, Y.; King, M.T.; Veech, R.L. A Dietary Ketone Ester Normalizes Abnormal Behavior in a Mouse Model of Alzheimer's Disease. *Int. J. Mol. Sci.* **2020**, *21*, doi:10.3390/IJMS21031044.

53. Marosi, K.; Kim, S.W.; Moehl, K.; Scheibye-Knudsen, M.; Cheng, A.; Cutler, R.;

Camandola, S.; Mattson, M.P. 3-Hydroxybutyrate Regulates Energy Metabolism and Induces BDNF Expression in Cerebral Cortical Neurons. *J. Neurochem.* **2016**, *139*, 769–781, doi:10.1111/JNC.13868.

54. Fortin, D.A.; Srivastava, T.; Dwarakanath, D.; Pierre, P.; Nygaard, S.; Derkach, V.A.; Soderling, T.R. Brain-Derived Neurotrophic Factor Activation of CaM-Kinase Kinase via Transient Receptor Potential Canonical Channels Induces the Translation and Synaptic Incorporation of GluA1-Containing Calcium-Permeable AMPA Receptors. *J. Neurosci.* **2012**, *32*, 8127–8137, doi:10.1523/JNEUROSCI.6034-11.2012.

55. Xu, Y.; Jiang, C.; Wu, J.; Liu, P.; Deng, X.; Zhang, Y.; Peng, B.; Zhu, Y. Ketogenic Diet Ameliorates Cognitive Impairment and Neuroinflammation in a Mouse Model of Alzheimer's Disease. *CNS Neurosci. Ther.* **2021**, doi:10.1111/CNS.13779.

56. Shippy, D.C.; Wilhelm, C.; Viharkumar, P.A.; Raife, T.J.; Ulland, T.K. β-Hydroxybutyrate Inhibits Inflammasome Activation to Attenuate Alzheimer's Disease Pathology. *J. Neuroinflammation* **2020**, *17*, doi:10.1186/s12974-020-01948-5.

57. Phillips, M.C.L. Fasting as a Therapy in Neurological Disease. *Nutrients* **2019**, *11*, doi:10.3390/nu11102501.

58. Włodarek, D. Role of Ketogenic Diets in Neurodegenerative Diseases (Alzheimer's Disease and Parkinson's Disease). *Nutrients* **2019**, *11*, doi:10.3390/NU11010169.

59. Parcerisas, A.; Pujadas, L.; Ortega-Gascó, A.; Perelló-Amorós, B.; Viais, R.; Hino, K.; Figueiro-Silva, J.; La Torre, A.; Trullás, R.; Simó, S.; et al. NCAM2 Regulates Dendritic and Axonal Differentiation through the Cytoskeletal Proteins MAP2 and 14-3-3. *Cereb. Cortex* **2020**, *30*, 3781–3799, doi:10.1093/CERCOR/BHZ342.

60. Fosch, A.; Rodriguez-Garcia, M.; Miralpeix, C.; Zagmutt, S.; Larrañaga, M.; Reguera, A.C.; Garcia-Chica, J.; Herrero, L.; Serra, D.; Casals, N.; et al. Central Regulation of Brown Fat Thermogenesis in Response to Saturated or Unsaturated Long-Chain Fatty Acids. *Int. J. Mol. Sci.* **2023**, *24*, doi:10.3390/IJMS24021697.

61. Casas, M.; Fadó, R.; Domínguez, J.L.; Roig, A.; Kaku, M.; Chohnan, S.; Solé, M.; Unzeta, M.; Miñano-Molina, A.J.; Rodríguez-Álvarez, J.; et al. Sensing of Nutrients by CPT1C Controls SAC1 Activity to Regulate AMPA Receptor Trafficking. *J. Cell Biol.* **2020**, *219*, doi:10.1083/JCB.201912045.

62. Fadó, R.; Soto, D.; Miñano-Molina, A.J.; Pozo, M.; Carrasco, P.; Yefimenko, N.; Rodríguez-Álvarez, J.; Casals, N. Novel Regulation of the Synthesis of α-Amino-3-Hydroxy-5-Methyl-4-Isoxazolepropionic Acid (Ampa) Receptor Subunit Glua1 by Carnitine Palmitoyltransferase 1C (CPT1C) in the Hippocampus. *J. Biol. Chem.* **2015**, *290*, 25548–25560, doi:10.1074/jbc.M115.681064.

63. Rothman, J.S.; Silver, R.A. NeuroMatic: An Integrated Open-Source Software Toolkit for Acquisition, Analysis and Simulation of Electrophysiological Data. *Front. Neuroinform.* **2018**, *12*, doi:10.3389/FNINF.2018.00014.

64. Griñán-Ferré, C.; Codony, S.; Pujol, E.; Yang, J.; Leiva, R.; Escolano, C.; Puigoriol-Illamola, D.; Companys-Alemany, J.; Corpas, R.; Sanfeliu, C.; et al. Pharmacological Inhibition of Soluble Epoxide Hydrolase as a New Therapy for Alzheimer's Disease. *Neurotherapeutics* **2020**, *17*, 1825–1835, doi:10.1007/S13311-020-00854-1.

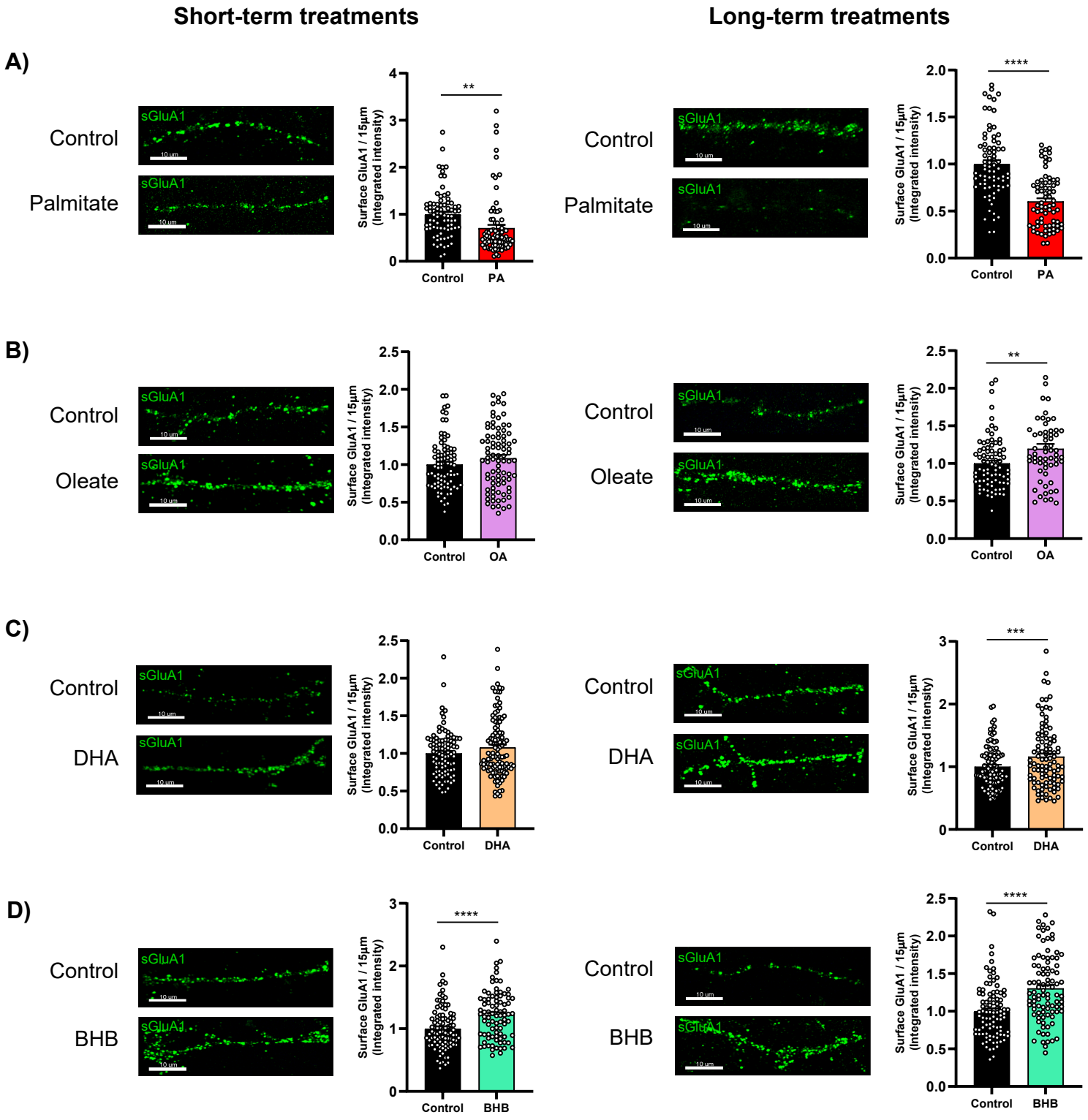
Short-term treatments
Long-term treatments
A)
Control
Palmitate
sGluA1
10 um
Surface GluA1 / 15µm (Integrated intensity)
Control
PA
**
****
B)
Control
Oleate
OA
C)
DHA
***
D)
BHB

**Figure 1**

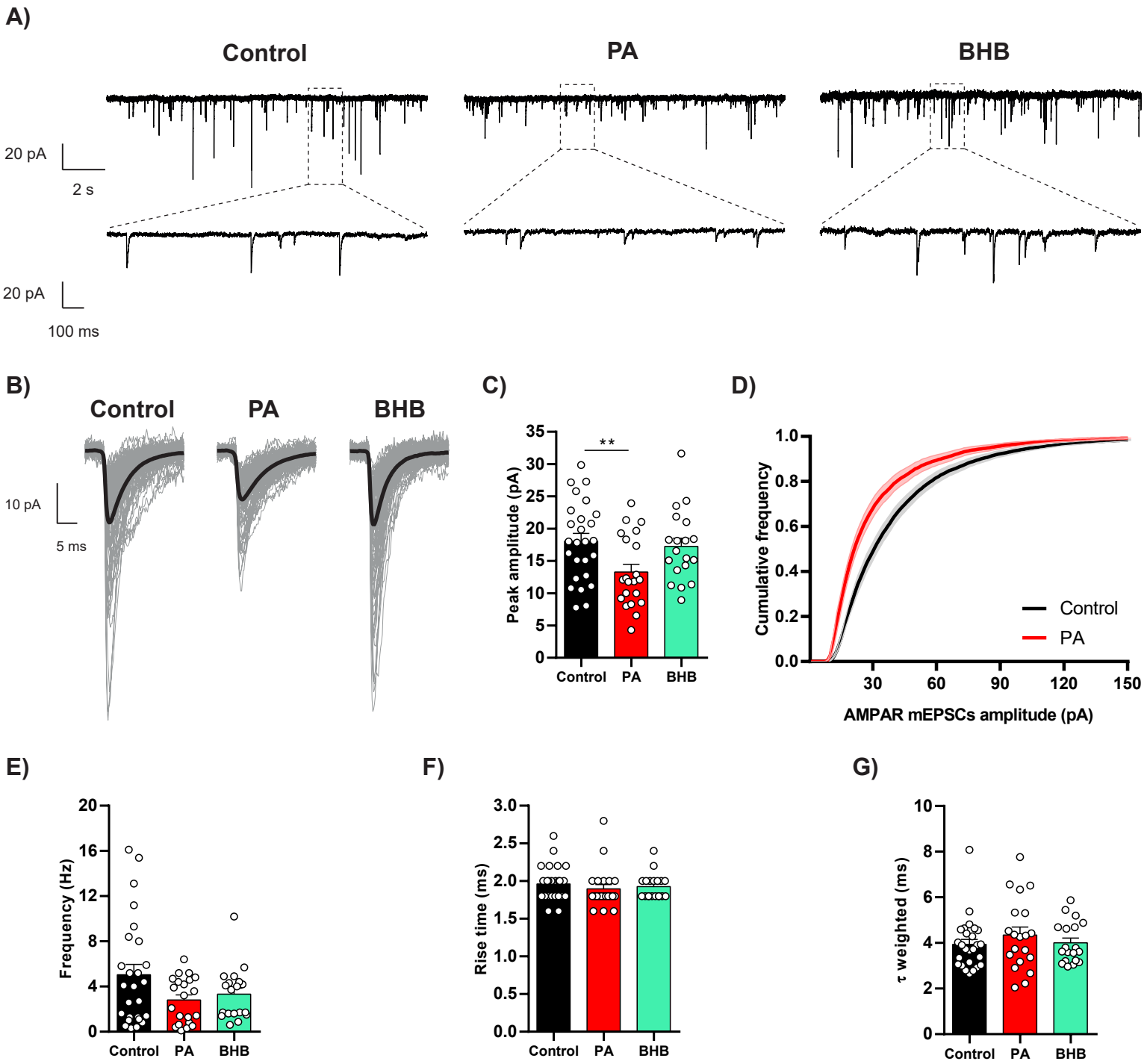
A)
Control
PA
BHB
20 pA
2 s
20 pA
100 ms
B)
Control
PA
BHB
10 pA
5 ms
C)
Peak amplitude (pA)
**
Control
PA
BHB
D)
Cumulative frequency
Control
PA
AMPAR mEPSCs amplitude (pA)
E)
Frequency (Hz)
Control
PA
BHB
F)
Rise time (ms)
Control
PA
BHB
G)
τ weighted (ms)
Control
PA
BHB

Figure 2

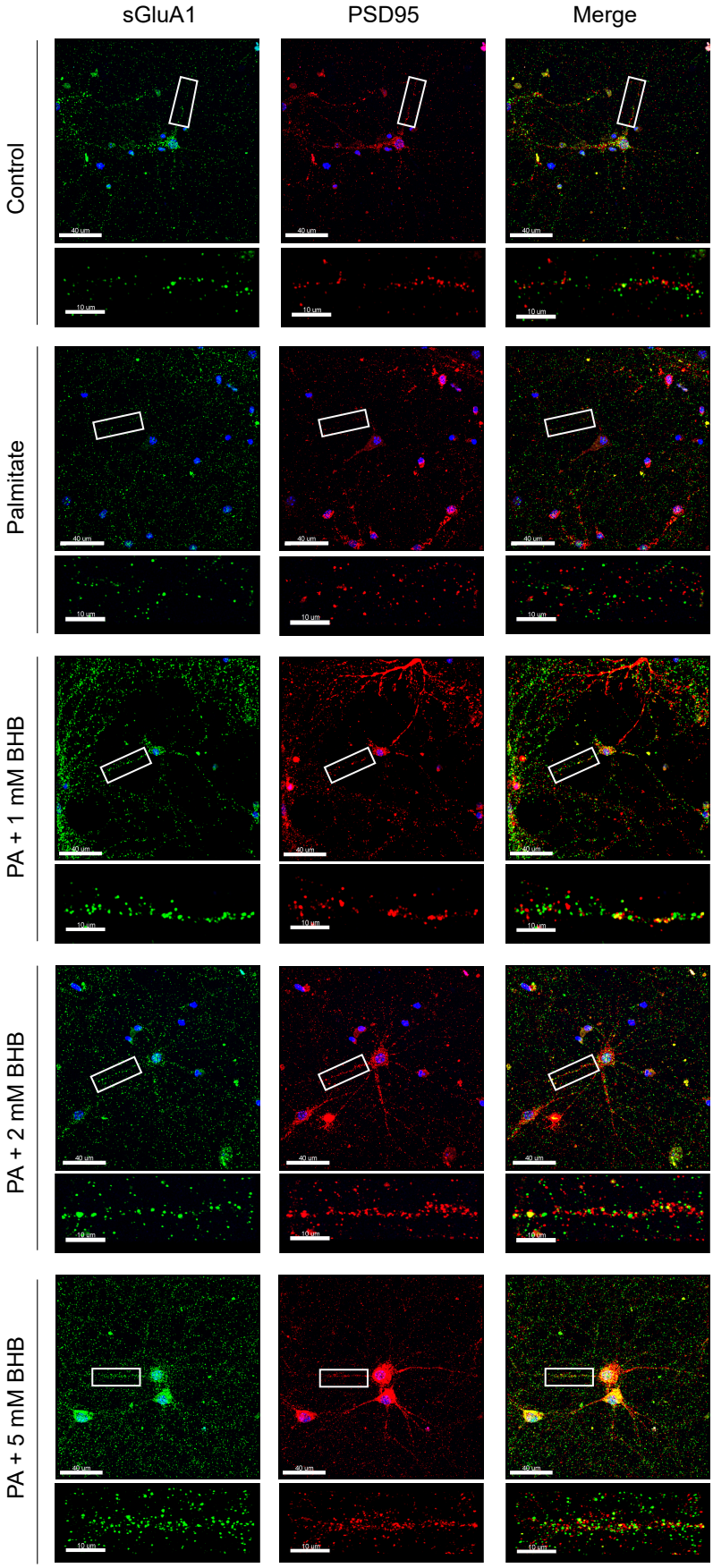
sGluA1
PSD95
Merge
Control
Palmitate
PA + 1 mM BHB
PA + 2 mM BHB
PA + 5 mM BHB

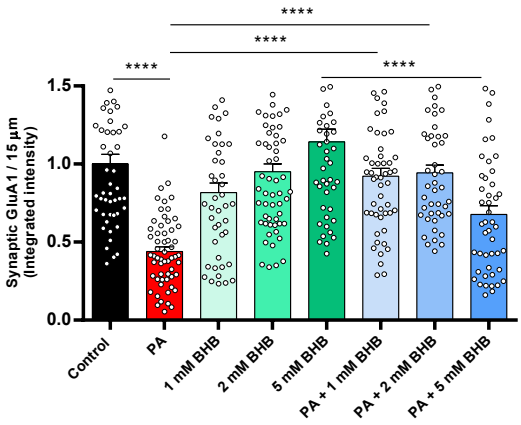
****
****
****
****
Synaptic GluA1 / 15 µm
(Integrated intensity)
1.5
1.0
0.5
0.0
Control
PA
1 mM BHB
2 mM BHB
5 mM BHB
PA + 1 mM BHB
PA + 2 mM BHB
PA + 5 mM BHB

**Figure 3**

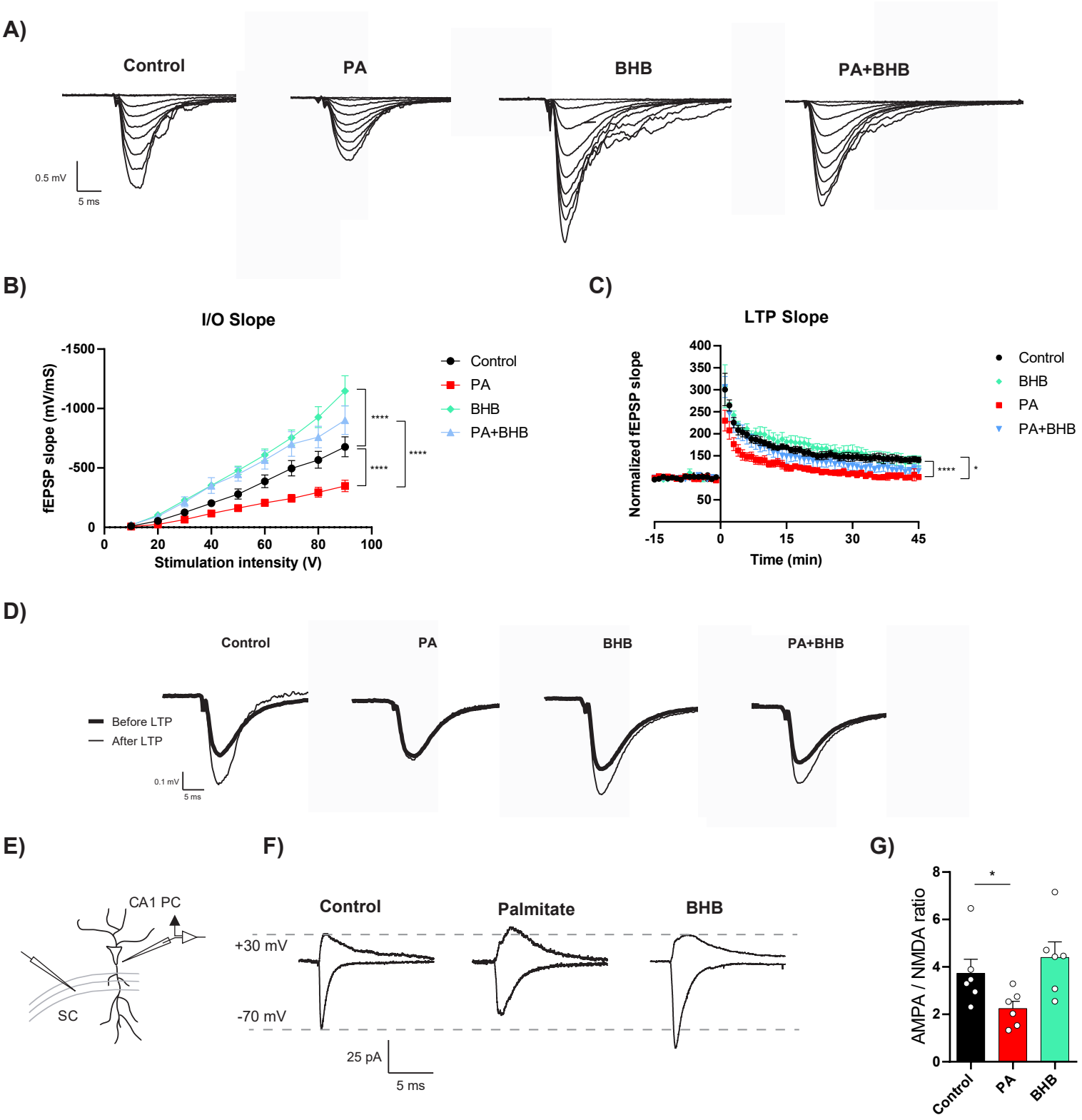
A)
Control
PA
BHB
PA+BHB
0.5 mV
5 ms
B)
I/O Slope
fEPSP slope (mV/mS)
-1500
-1000
-500
0
0
20
40
60
80
100
Stimulation intensity (V)
Control
PA
BHB
PA+BHB
****
****
****
C)
LTP Slope
Normalized fEPSP slope
400
350
300
250
200
150
50
-15
0
15
30
45
Time (min)
Control
BHB
PA
PA+BHB
****
*
D)
Control
PA
BHB
PA+BHB
Before LTP
After LTP
0.1 mV
5 ms
E)
CA1 PC
SC
F)
Control
Palmitate
BHB
+30 mV
-70 mV
25 pA
5 ms
G)
AMPA / NMDA ratio
8
6
4
2
0
*
Control
PA
BHB

Figure 4

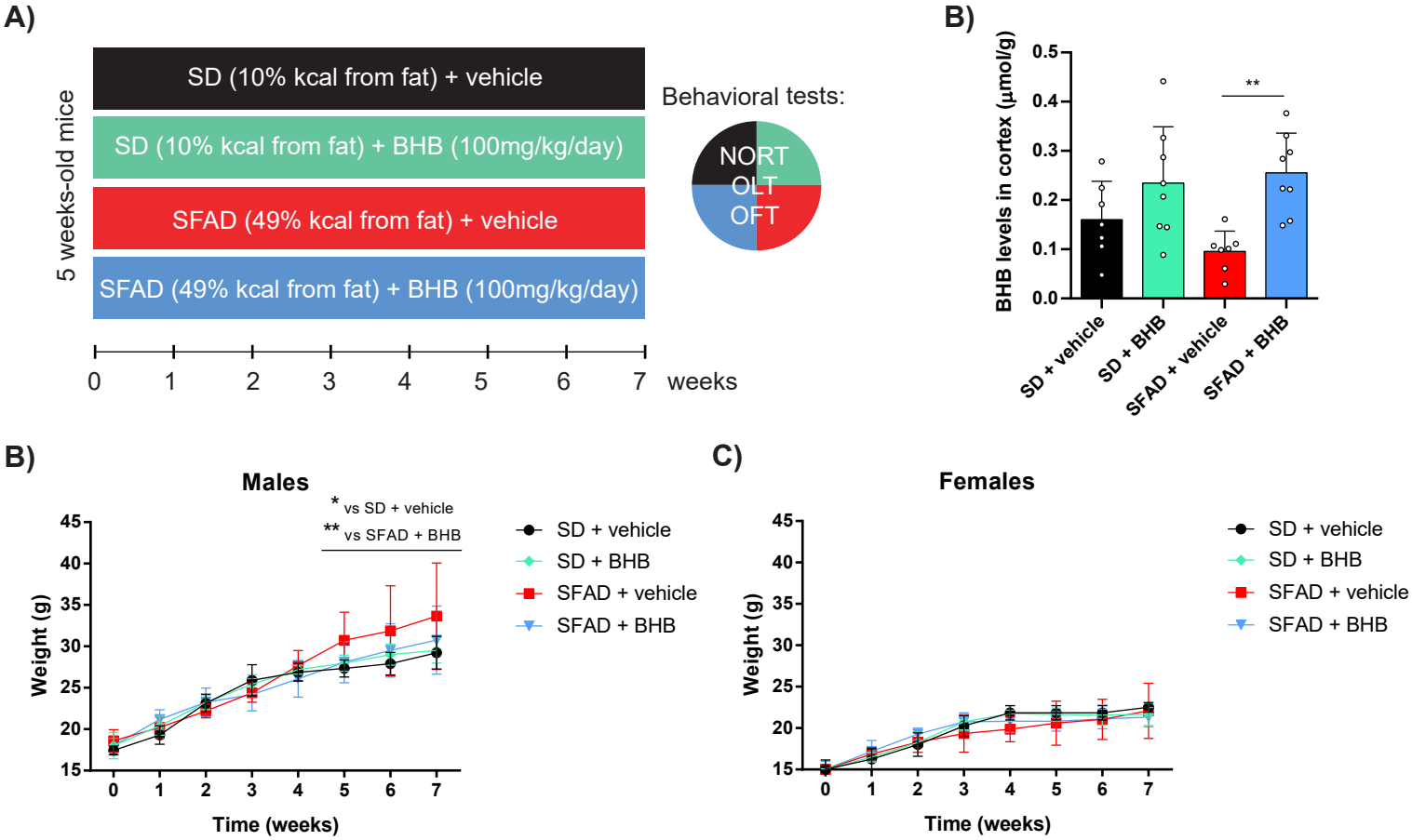
A)
5 weeks-old mice
SD (10% kcal from fat) + vehicle
SD (10% kcal from fat) + BHB (100mg/kg/day)
SFAD (49% kcal from fat) + vehicle
SFAD (49% kcal from fat) + BHB (100mg/kg/day)
0 1 2 3 4 5 6 7 weeks
Behavioral tests:
NORT
OLT
OFT
B)
BHB levels in cortex (µmol/g)
0.0 0.1 0.2 0.3 0.4 0.5
**
SD + vehicle
SD + BHB
SFAD + vehicle
SFAD + BHB
B)
Males
* vs SD + vehicle
** vs SFAD + BHB
Weight (g)
15 20 25 30 35 40 45
0 1 2 3 4 5 6 7
Time (weeks)
SD + vehicle
SD + BHB
SFAD + vehicle
SFAD + BHB
C)
Females
Weight (g)
15 20 25 30 35 40 45
0 1 2 3 4 5 6 7
Time (weeks)
SD + vehicle
SD + BHB
SFAD + vehicle
SFAD + BHB

**Figure 5**

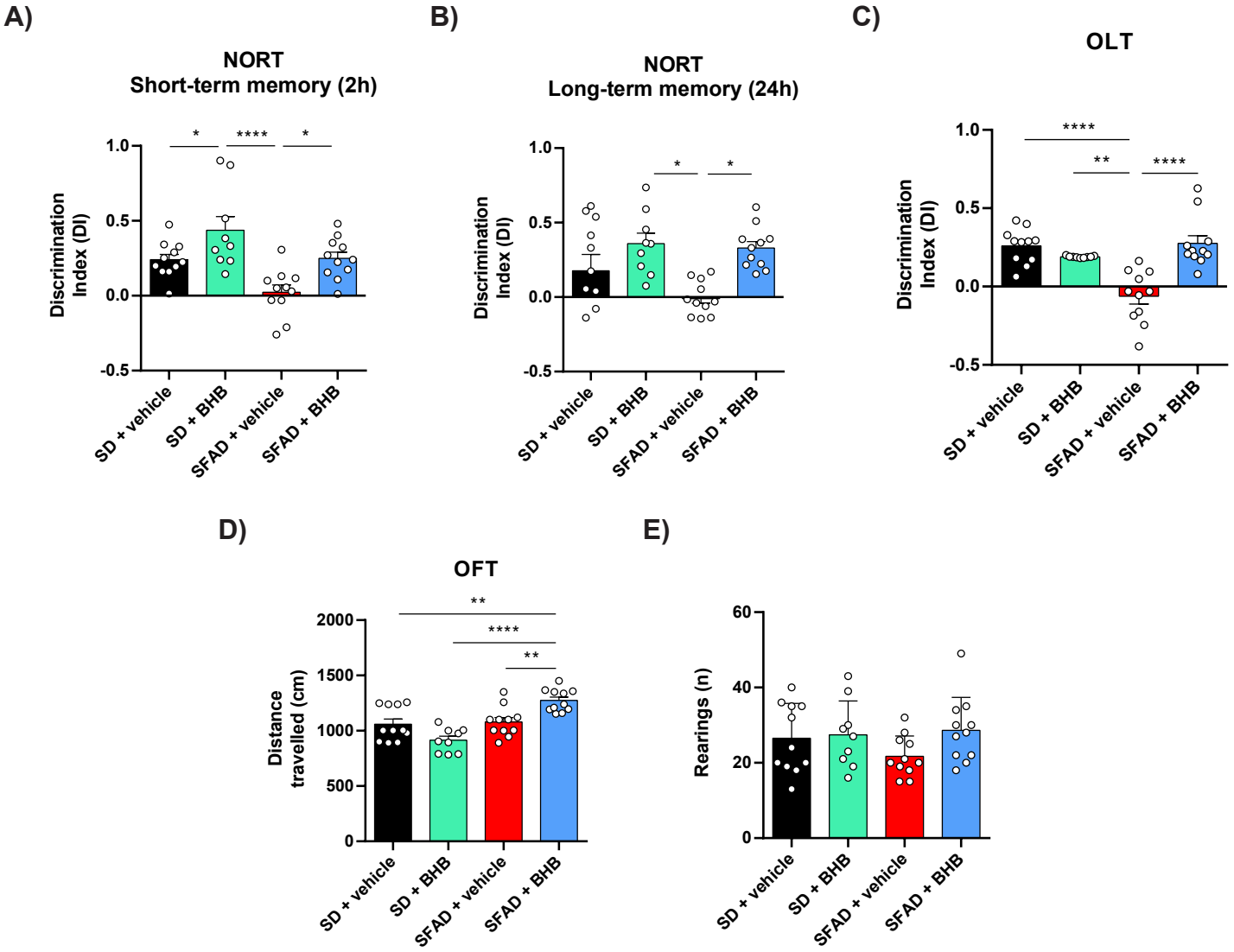
A)
NORT
Short-term memory (2h)
Discrimination Index (DI)
1.0
0.5
0.0
-0.5
*
****
*
SD + vehicle
SD + BHB
SFAD + vehicle
SFAD + BHB
B)
NORT
Long-term memory (24h)
Discrimination Index (DI)
1.0
0.5
0.0
-0.5
*
*
SD + vehicle
SD + BHB
SFAD + vehicle
SFAD + BHB
C)
OLT
Discrimination Index (DI)
1.0
0.5
0.0
-0.5
****
**
****
SD + vehicle
SD + BHB
SFAD + vehicle
SFAD + BHB
D)
OFT
Distance travelled (cm)
2000
1500
1000
500
0
**
****
**
SD + vehicle
SD + BHB
SFAD + vehicle
SFAD + BHB
E)
Rearings (n)
60
40
20
0
SD + vehicle
SD + BHB
SFAD + vehicle
SFAD + BHB

**Figure 6**